

1 **Influence of climate variability, fire and phosphorus limitation on the**  
2 **vegetation structure and dynamics in the Amazon-Cerrado border**

3

4 Emily Ane Dionizio da Silva<sup>1</sup>, Marcos Heil Costa<sup>1</sup>, Andrea Almeida Castanho<sup>2</sup>, Gabrielle Ferreira Pires<sup>1</sup>,  
5 Beatriz Schwantes Marimon<sup>3</sup>, Ben Hur Marimon-Junior<sup>3</sup>, Eddie Lenza<sup>3</sup>, Fernando Martins Pimenta<sup>1</sup>,  
6 Xiaojuan Yang<sup>4</sup>, Atul K. Jain<sup>5</sup>

7

8 <sup>1</sup> Department of Agricultural Engineering, Federal University of Viçosa (UFV), Viçosa, MG, Brazil

9 <sup>2</sup> The Woods Hole Research Center, 149 Woods Hole Rd., Falmouth, MA USA

10 <sup>3</sup> Federal University of Mato Grosso, Nova Xavantina Campus, Nova Xavantina, MT, Brazil

11 <sup>4</sup> Oak Ridge National Laboratory, Oak Ridge, TN, USA


12 <sup>5</sup> Department of Atmospheric Sciences, University of Illinois at Urbana-Champaign

13

14 Correspondence to: Emily Ane D. da Silva (emilyy.ane@gmail.com)

15

16 **Abstract**

17 Climate, fire and soil nutritional limitation are important elements that affect the vegetation  
18 dynamics in areas of forest-savanna transition. In this paper, we use the dynamic vegetation model  
19 INLAND to evaluate the influence of inter-annual climate variability, fire and phosphorus (P) limitation  
20 on the Amazon-Cerrado transitional vegetation structure and dynamics. We assess how each  
21 environmental factor affects the net primary production, leaf area index and aboveground biomass (AGB),  
22 and compare the AGB simulations  of observed AGB map. We used two regional datasets – the 1961-  
23 1990 average seasonal climate and the 1948 to 2008 inter-annual climate variability, two datasets of total  
24 soil P content in soil, based on regional (field measurements) and global data and the INLAND fire  
25 module. Our results show that inter-annual climate variability, P limitation and fire occurrence gradually  
26 improve simulated vegetation types and these effects are not homogeneous along the  
27 latitudinal/longitudinal gradient showing a synergistic effect among them. In terms of magnitude, the  
28 effect of fire is stronger, and is the main driver of vegetation changes along the transition. The nutritional  
29 limitation, in turn, is stronger than the effect of inter-annual climate variability acting on the transitional  
30 ecosystems dynamics. Overall, INLAND typically simulates more than 80% of the AGB variability in  
31 the transition zone. However, the AGB in many places is clearly not well simulated, indicating that  
32 important soil and physiological factors in the Amazon-Cerrado border, such as lithology and water table  
33 depth, carbon allocation strategies and mortality rates, still need to be included in the model.

## 34 **1 Introduction**



35         The Amazon and Cerrado are the two largest and most important phytogeographical domains in  
36 South America. The Amazon forest has been globally recognized and distinguished not only for its  
37 exuberance in diversity and species richness, but also for playing an important role in the global climate  
38 by regulating water (Bonan, 2008; Pires and Costa, 2013) and heat fluxes (Shukla et al., 1990; Rocha et  
39 al., 2004; Roy et al., 2002). The Cerrado is recognized worldwide for being the richest savanna in the  
40 world (Myers et al., 2000; Klink and Machado, 2005). It is characterized by different physiognomies,  
41 ranging from sparse physiognomies to dense woodland formations, and the latter are commonly mixed  
42 with Amazon rainforest forming transitional areas. The Amazon-Cerrado transition extends for 6270 km  
43 from northeast to southwest in Brazil, and the ecotonal vegetation around this transition is a mix of the  
44 characteristics of the tropical forest and the savanna (Torello-Raventos et al., 2013).

45         Gradients of seasonal rainfall and water deficit, fire occurrence, herbivory and low fertility of the  
46 soil have been reported as the main factors that characterize the transition between forest and savanna  
47 globally (Lehmann et al., 2011; Hoffman et al., 2012; Murphy and Bowman, 2012). However, few studies  
48 have evaluated the individual and combined effects of these factors on Brazilian ecosystems ecotones  
49 (Marimon-Junior and Haridasan, 2005; Elias et al., 2013; Vourtilis et al., 2013).

50         It is challenging to assess the degree of interaction among these various environmental factors in  
51 the transitional region and to infer how each one influences the distribution of the regional vegetation. In  
52 this case, Dynamic Global Vegetation Models (DGVMs) can be powerful tools to isolate the influences  
53 of climate, fire and nutrients, therefore helping to understand their large-scale effects on vegetation  
54 (House et al., 2003; Favier et al., 2004; Hirota et al., 2010; Hoffman et al., 2012).

55 Previous modelling studies using DGVMs that investigate climate effects in the Amazon indicate  
56 that the rainforest could experience changes in rainfall patterns which would either transform the forest  
57 into an ecosystem with more sparse vegetation – similar to a savanna, what has been called as the  
58 "savannization of the Amazon" (Shukla et al., 1990; Cox et al., 2000; Oyama and Nobre, 2003; Betts et  
59 al., 2004; Cox et al., 2004; Salazar et al., 2007) - or to a seasonal forest (Malhi et al., 2009; Pereira et al.,  
60 2012; Pires and Costa, 2013). These studies had great importance to the improvement of terrestrial  
61 biosphere modeling, but they neglect two important processes in tropical ecosystem dynamics: fire  
62 occurrence and nutrient limitation, particularly the Phosphorus (P) limitation.

63 In tropical ecosystems, fire plays an important ecological role and influences the productivity, the  
64 biogeochemical cycles and the dynamics in the transitional biomes, not only by changing the phenology  
65 and physiology of plants, but also by modifying the competition among trees and lower canopy plants  
66 such as grasses, shrubs and lianas. Fire occurrence, depending on its frequency and intensity, may increase  
67 the mortality of trees and transform an undisturbed forest into a disturbed and flammable one (House et  
68 al., 2003; Hirota et al., 2010; Hoffmann et al., 2012). Fires also affect the dynamics of nutrients in the  
69 savanna ecosystem, changing mainly the N:P relationship and P availability in the soil (Nardoto et al.  
70 2006).

71 Studies suggest that P is the main limiting nutrient within tropical forests (Malhi et al., 2009;  
72 Mercado et al., 2011; Quesada et al., 2012)  unlike the temperate forests. Phosphorus is a nutrient that is  
73 easily  adsorbed by soil minerals due to the large amount of iron and aluminum oxides in the Amazon  
74 and Cerrado acidic and strongly weathered soils (Dajoz, 2005; Goedert, 1986). In the tropics, the warm  
75 and wet climate favors the high biological activity in the soil and the litter decomposition, not limiting

76 the nitrogen for plant fixation. In Cerrado, higher soil fertility is related to regions with greater woody  
77 plants abundance and less grass cover, similarly to the features found in the Amazon rainforest (Moreno  
78 et al., 2008; Vourtilis et al., 2013; Veenendaal et al., 2015). However, the phosphorus limitation is often  
79 neglected by DGVMs. which usually assume unlimited P availability and consider nitrogen as the main  
80 limiting nutrient. However, N is not a limiting nutrient for trees in the tropics (Davidson et al. 2004),  
81 while P availability affects the trees dynamics.

82 In principle, in transitional forests, where the climate is intermediate between wet and seasonally  
83 dry, the heterogeneous structure and phenology make it difficult to represent these forests in models. The  
84 Amazon-Cerrado border is the result of the expansion and contraction of the Cerrado into the forest (see  
85 Marimon et al., 2006; Morandi et al., 2016), especially in the Mato Grosso state, where extreme events,  
86 such as intense droughts, influence the vegetation dynamics (Marimon et al., 2014) and the nutrient  
87 (Oliveira et al., 2017) and carbon cycling (Valadão et al., 2016).

88 Currently, no model has demonstrated to be able to accurately simulate the vegetation transition  
89 between Amazon and Cerrado. In general the DGVMs simulate evergreen forest along the Amazon-  
90 Cerrado border and neglect savanna occurrence (Botta and Foley, 2002; Bond et al., 2005; Salazar et al.,  
91 2007; Smith et al., 2014). This difficulty may be due to absence or not well represented disturbances such  
92 as fire, nutritional limitation or soil proprieties. Thus, we need a better understanding of the drivers on  
93 transitional vegetation to determine the parameters and establish relations between the environmental and  
94 transitional vegetation physiognomies.

95 In this paper we use the dynamic vegetation model INLAND (Integrated Model of Land Surface  
96 Processes) to evaluate the influence of inter-annual climate variability, fire occurrence and P limitation

97 in the Amazon-Cerrado transitional vegetation dynamics and structure. We assess how each element  
98 affects the net primary production (NPP), leaf area index (LAI) and aboveground biomass (AGB) and  
99 compare the model simulated AGB to observed AGB data. The results presented here are important to  
100 build models that accurately represent the transition vegetation, and show the need to include the spatial  
101 variability of eco-physiological parameters in these areas.

## 102 **2 Materials and methods**

### 103 **2.1 Study Area**

104 The present study focuses on the Amazon-Cerrado transition (Figure 1). We use the official  
105 delimitation of the Brazilian biomes proposed by IBGE (2004), and define five transects along the  
106 transition border with  $1^\circ \times 1^\circ$  grid size (the terms “transition”, “Amazon-Cerrado transition” and “Forest-  
107 Savanna transition” are used interchangeably with the same meaning throughout this  
108 manuscript). Transects 1 to 4 are established considering approximately 330 km into the Amazon and 330  
109 km into the Cerrado domain, while Transect 5 is 880 km long on the southern Amazon-Cerrado border.  
110 The transects are located as follows: Transect 1 (T1,  $44^\circ$ -  $50^\circ$ W;  $5^\circ$ -  $7^\circ$ S), Transect 2 (T2,  $46^\circ$ - $51^\circ$  W;  $7^\circ$ -  
111  $9^\circ$ S), Transect 3 (T3,  $48^\circ$ - $54^\circ$  W;  $9^\circ$ - $11^\circ$  S), Transect 4 (T4,  $49^\circ$  -  $55^\circ$  W;  $11^\circ$ - $13^\circ$  S), and Transect 5 (T5,  
112  $52^\circ$  -  $60^\circ$  W;  $13^\circ$ - $15^\circ$  S) (Figure 1).

### 113 **2.2 Description of the INLAND Surface Model**

114 The Integrated Model of Land Surface Processes (INLAND) is the land-surface component of the  
115 Brazilian Earth System Model (BESM). INLAND is basically a revision of the IBIS model (Integrated  
116 Biosphere Simulator, described by Foley et al., 1996; Kucharik et al., 2000), through assembly and

117 standardization of different IBIS versions, and improvements in software engineering. We used the  
118 version described by Senna et al. (2009) as starting point for INLAND. No changes in tuning were done  
119 since that paper, except the addition of the P parameterization, described below. Code is available from  
120 <http://www.biosfera.dea.ufv.br/en-US/download-inland>.

121 The model considers changes in the composition and structure of vegetation in response to the  
122 environment and incorporates important aspects of biosphere-atmosphere interactions. The model  
123 simulates the exchanges of energy, water, carbon and momentum between soil-vegetation-atmosphere.  
124 These processes are organized in a hierarchical framework and operate at different time steps, ranging  
125 from 60 minutes to 1 year, coupling ecological, biophysical and physiological processes. The vegetation  
126 structure is represented by two layers: upper (arboreal PFTs) and lower (no arboreal PFTs, shrubs and  
127 grasses) canopies, and the composition is represented by 12 plant functional types (PFTs) (e.g., tropical  
128 broadleaf evergreen trees or C4 grasses, among several others).The photosynthesis and respiration  
129 processes are simulated in a mechanistic manner using the Ball-Berry-Farquhar model (details in Foley  
130 et al., 1996). The vegetation phenology module simulates the processes such as budding and senescence  
131 based on drought phenology scheme for tropical deciduous trees. The dynamic vegetation module  
132 computes the following variables yearly for each PFT: gross and net primary productivity (GPP and NPP),  
133 changes in AGB pools, simple mortality disturbance processes and resultant LAI, thus allowing  
134 vegetation type and cover to change with time. The partitioning of the NPP for each PFT resolves carbon  
135 in three AGB pools: leaves, stems and fine roots. The LAI of each PFT is obtained by simply dividing  
136 leaf carbon by specific leaf area, which in INLAND is considered fixed (one value) for each PFT.

137 INLAND has eight soil layers to simulate the diurnal and seasonal variations of heat and moisture.  
138 Each layer is described in terms of soil temperature, volumetric water content and ice content (Foley et  
139 al., 1996; Thompson and Pollard, 1995). Furthermore, all of these processes are influenced by soil texture  
140 and amount of organic matter within the soil profile.

141 Considering these aspects of vegetation dynamics and soil physical properties the model can  
142 simulate plant competition for light and water between trees, shrubs and grasses through shading and  
143 differences in water uptake (Foley et al., 1996). These PFTs can coexist within a grid cell and their annual  
144 LAI values indicate the dominant vegetation type within a grid cell. For example, the dominant vegetation  
145 type is a Tropical Evergreen Forest if the PFT tropical broadleaf evergreen tree has an annual mean upper  
146 canopy LAI ( $LAI_{upper}$ ) above  $2.5 \text{ m}^2 \text{ m}^{-2}$ . On the other hand, the dominant vegetation type is a Tropical  
147 Deciduous Forest if the tropical broadleaf drought-deciduous tree has an annual mean  $LAI_{upper}$  above  
148  $2.5 \text{ m}^2 \text{ m}^{-2}$ . Where total tree LAI ( $LAI_{upper}$ ) is between  $0.8$  and  $2.5 \text{ m}^2 \text{ m}^{-2}$ , dominant vegetation type is  
149 savanna, and  $LAI_{upper}$  values smaller than  $0.8 \text{ m}^2 \text{ m}^{-2}$  characterize a grassland vegetation type.

150 We assume that the vegetation types Tropical Evergreen Forest and the Tropical Deciduous Forest  
151 in INLAND represents the Amazon rainforest, while Savanna and Grasslands represent the Cerrado.  
152 Savanna would be equivalent to the Cerrado physiognomies *Cerradão* and *Cerrado sensu strictu*, while  
153 Grasslands would be equivalent to the physiognomies *Campo sujo* and *Campo Limpo* (*sensu* Ribeiro and  
154 Walter, 2008).

155 The soil chemical properties are represented by the carbon, nitrogen and phosphorus. The carbon  
156 cycle is simulated through vegetation, litter and soil organic matter, where the biogeochemical module is  
157 similar to the CENTURY model (Parton et al., 1993; Verberne et al., 1990). The amount of C existing in



158 the first meter of soil is divided into different compartments characterized by their residence time, which  
159 can vary in an interval of hours for microbial AGB and organic matter to several years for lignin. The  
160 model considers only the soil N transformations and carbon decomposition, but the N cycle is not fully  
161 simulated and N does not influence the vegetation productivity, i.e., there is a fixed C:N ratio. The P cycle  
162 also is not fully implemented, instead the P-limitation is spatially parameterized through the linear relation  
163 developed by Castanho et al. (2013) to limit the gross primary productivity. A map of total P available in  
164 the soil ( $P_{total}$ ) is used by the model to estimate the maximum capacity of carboxylation by the Rubisco  
165 enzyme ( $V_{max}$ ) for each grid using Equation (1) :

$$166 \quad V_{max} = 0.1013 P_{total} + 30.037 \quad (1)$$

167 where  $V_{max}$  and  $P_{total}$  are given in  $\mu\text{molCO}_2 \text{ m}^{-2} \text{ s}^{-1}$  and  $\text{mg kg}^{-1}$ , respectively. This equation has been based  
168 on data for tropical evergreen and deciduous trees, and is applied only to these two PFTs, the other PFTs  
169 are unaffected.

170 INLAND also contains a spatial fire module, based on the Canadian Terrestrial Ecosystem Model  
171 CTEM (Arora and Boer, 2005). In this module, three aspects of the fire triangle are considered – the  
172 availability of fuel to burn, the flammability of vegetation, and the presence of an ignition source. Each  
173 is represented daily by an independently calculated probability and the product of the three is the  
174 probability of fire occurrence, calculated daily. Availability of fuel to burn depends on biomass,  
175 flammability depends on soil moisture and ignition depends on a random lightning occurrence and a  
176 constant anthropogenic ignition probability. The daily fire occurrence probability is equal to the daily  
177 AGB burned fraction. The AGB burned fraction is accumulated throughout the year and its ratio is applied  
178 at the end of each year to the grid cell area, reducing the leaf, wood and root biomass pools.

## 179 2.3 Observed data

### 180 2.3.1 Phosphorus databases

181 We used two P databases to estimate  $V_{\max}$  (Equation 1): one regional (referred to as PR) and one  
182 global database referred to as PG). In addition, a control P map (PC) represents the unlimited nutrient  
183 availability case, equivalent to a  $V_{\max}$  of  $65 \mu\text{molCO}_2 \text{ m}^{-2} \text{ s}^{-1}$ , or  $350 \text{ mg P kg}^{-1}$  soil, according to Equation  
184 1.

185 The PR database was developed from total P in the soil for the Amazon basin published by  
186 Quesada et al. (2011) plus 54 additional available P samples (P extracted via Mehlich-1 extractor,  
187  $P_{\text{mehlich-1}}$ ) (Figure 2a). We used the  $P_{\text{mehlich-1}}$  and clay contents measured in a forest-savanna transition  
188 region in Brazil (Mato Grosso state) to estimate  $P_{\text{total}}$  and expand the coverage area of the P data (Section  
189 S1). These 54 samples were gridded to a  $1^\circ \times 1^\circ$  grid to be compatible with the spatial resolution used by  
190 INLAND, resulting in 12 additional pixels with observed total P content (Figure 2a). For pixels without  
191 observed  $P_{\text{total}}$ , the  $P_{\text{total}}$  was assumed to be  $350 \text{ mg P kg}^{-1}$  soil, similarly to the PC conditions.

192 A global dataset of  $P_{\text{total}}$  (Figure 2b) was also used to estimate  $V_{\max}$ . This global data set is part of  
193 a database containing six global maps of the different forms of P in the soil (Yang et al., 2013). The  $P_{\text{total}}$   
194 was estimated from lithologic maps, distribution of soil development stages, fraction of the remaining  
195 source material for different stages of weathering using chronosequence studies (29 studies), and P  
196 distribution in different forms for each soil type based on the analysis of Hedley fractionation (Yang and  
197 Post, 2011), which are part of a worldwide collection of soil profile data. The uncertainties and limitations  
198 associated with this database are restricted to the Hedley fractionation data used, which are 17% for low  
199 weathered soils, 65% for intermediate soils and 68% for highly weathered soils (Yang et al., 2013).

### 200 2.3.2 Above-Ground Biomass (AGB) database



201 The AGB database used was created by Nogueira et al. (2015) and considered undisturbed (pre-  
202 deforestation) vegetation existing in the Brazilian Amazonia. This database was compiled from a  
203 vegetation map at a scale of 1:250000 (IBGE, 1992) and AGB averages from 41 published studies that  
204 had conducted direct sampling in either forest (2317 plots) or non-forest or contact zones (1830 plots).  
205 We bi-linearly interpolated the AGB (dry weight) for each transect considering  $1^\circ \times 1^\circ$  to ensure  
206 compatibility of the observed and simulated data.

207 Five longitudinal transects (Figure 1) were individually used to characterize AGB in the Amazon-  
208 Cerrado border (Figures 3a and 3b). In T1, T2, T3 and T4, the higher AGB values in the west and lower  
209 values in the east are consistent with the transition from a dense and woody vegetation (the Amazon  
210 forest) towards a sparse vegetation with lower AGB (the Cerrado). However, T1 shows a more gradual  
211 reduction of AGB along the west to east gradient, while in T2, T3 and T4 where the transition is more  
212 abrupt. In T5 no west-east gradient is present with high AGB heterogeneity and predominant low AGB  
213 across the transect (Figure 3b).

214

### 215 2.4 Simulations

216 The model was forced with the prescribed climate data based on the Climate Research Unit (CRU)  
217 database (Harris et al., 2014). Two climate boundary conditions were used: the first is referred to as the  
218 monthly climatological average (CA) that represents the average climate for the period 1961-1990. The  
219 second climate boundary condition is the historical dataset, for the continuous period between 1948 and  
220 2008, thus considering interannual climate variability (CV). For both boundary conditions, the variables

221 used are rainfall, solar radiation, wind velocity and maximum and minimum temperatures. The CRU  
222 database is developed from observations at meteorological stations across the world's land areas and has  
223 been widely used by the scientific community in case studies to evaluate El Niño–Southern Oscillation  
224 (ENSO) effects and other modes of interannual climate variability (Foley et al., 2002; Marengo, 2004;  
225 Wang et al., 2014), because these data preserve the spatial mean of the rainfall data, although they do not  
226 provide adequate representation of the precipitation variance (Beguería et al., 2016). The dataset has a 1-  
227 degree spatial resolution and a monthly time resolution.

228 Soil texture data is based on the IGBP-DIS global soil (Global Soil Data Task 2000) (Hansen and  
229 Reed, 2000). In the CV group of runs, the model was spin-up by cycling the 1948-2008 climate data (61-  
230 year) seven times, totaling 427 years. In the CA group of runs, the annual mean climate data was cycled  
231 427 times. In both cases, CO<sub>2</sub> varied from 278 to 380 ppmv, according to observations in the period,  
232 updated annually. In both cases, only the model results of the last 10 years were used to analyze the  
233 results.

234 The experiment design is a factorial combination of the climate scenarios (CA, monthly  
235 climatological average, 1961-1990; CV, monthly climate time series, 1948-2008), the nutrient limitation  
236 on V<sub>max</sub> (PC, no P limitation ( $V_{\max} = 65 \mu\text{molCO}_2 \text{ m}^{-2} \text{ s}^{-1}$ ); PR, regional P limitation; PG, global P  
237 limitation) and the occurrence of fire (F) or not (Table 1). The 12 combinations in Table 1 allow the  
238 evaluation of individual and combined effects of climate, soil chemistry, and the incidence of fire on the  
239 variables: Net Primary Production (NPP), tree AGB, and LAI of the upper and lower canopies (LAI<sub>upper</sub>,  
240 LAI<sub>lower</sub>).

241 We consider that the subtraction between the simulations (CV+PC) and (CA+PC) represents the  
242 isolated effect of inter-annual climate variability without P limitations. The same logic is applied to isolate  
243 other factors such as fire and P in different climate scenarios. For example, the fire effect under average  
244 climate without P limitation case is calculated by the difference between CA+PC+F and CA+PC.  
245 Similarly, the isolated effect of fire under a climate with inter-annual variability scenario without  
246 influence of P limitation is calculated by the difference between CV+PC+F and CV+PC. The different  
247 combinations of climate scenarios with and without fire effects and with and without P limitations are  
248 described in Table 2.

## 249 **2.5 Statistical analysis and determination of the best model configuration**

250 The statistical analysis is divided in four parts. First, we present maps of the isolated effects for  
251 all simulated area calculated as the average of last ten years of simulated spatial patterns. The statistical  
252 significance of the isolated effects on NPP, LAI and AGB are determined using the t-test with  $p < 0.05$ .  
253 The results are tested in each pixel, for all the simulated domain ( $n = 10$ ).

254 Second, we present an analysis of variance using the one-way ANOVA and the Tukey-Kramer  
255 test in the transition zone. We consider all 31 pixels which fall in transects T1 to T5 ( $n_{\text{pixels}}$ ). The results  
256 presented are based on the set of last 10 years of simulation (1999-2008,  $n_{\text{years}}$ ) for the 12 combinations  
257 ( $n_{\text{simulation}}$ ) in Table 1. Moreover, we grouped treatments according to climate regardless of P limitation,  
258 presence or absence of fire, where all sets with CV vs CA are tested (Group 1,  $n=1860$ , ( $n_{\text{pixel}} \times n_{\text{year}} \times$   
259 ( $n_{\text{simulation}}/2$ )). Similarly, in Group 2 we tested if PC, PR or PG were significantly different from each other  
260 regardless the F or climate used (Group 2,  $n=1240$ , ( $n_{\text{pixel}} \times n_{\text{year}} \times (n_{\text{simulation}}/3)$ ). In Group 3 we tested if  
261 fire introduced a significant effect regardless of climate and P limitation (Group 3,  $n=1860$ , ( $n_{\text{pixel}} \times n_{\text{year}}$

262  $\times (n_{\text{simulation}}/2)$ ). Finally, all treatments were tested to each simulation assessing their individual effects on  
263 NPP, LAI and AGB ( $n_{\text{pixel}} \times n_{\text{year}} = 310$ ).

264 Third, a correlation coefficient between the simulated and observed values for AGB was  
265 calculated for each transect. The simulated variables are averaged for the last 10 years of simulations  
266 (1999 - 2008) and compared to AGB from Nogueira et al. (2015) within a grid cell.

267 Finally, we evaluate INLAND's ability to assign the dominant vegetation type by analyzing 10  
268 years of probability of occurrence. If the dominant vegetation type (evergreen tropical forest, or deciduous  
269 forest for the Amazon rainforest, and savanna or grasslands for Cerrado) in a pixel is the same in more  
270 than 90% of the simulated years (9 out of 10), then the simulated vegetation type is defined as "very  
271 robust" for that pixel; if it occurs in 70 - 90% of the simulated years, the simulated result is considered to  
272 be "robust". If the dominant vegetation occurred in less than 70% of simulated years, the pixel is  
273 considered "transitional" vegetation.

## 274 **3 Results**

### 275 **3.1 Influence of climate, fire and phosphorus in the Amazon-Cerrado transition region**

#### 276 **3.1.1 Spatial patterns**

277 Overall, the inclusion of inter-annual climate variability (CV) resulted in a decrease in the  
278 simulated average tree biomass (TB) by 3.8% in the entire Brazilian Amazonia, and by 8.7% in the entire  
279 Cerrado in comparison to average climate (CA), values obtained by difference  $CV+PC - CA+PC$  (Figure  
280 4a). The spatial differences between CV and CA for TB simulations are statistically significant and range  
281 from  $-3 \text{ kg-C m}^{-2}$  to  $+2 \text{ kg-C m}^{-2}$ . The state of Pará, with higher influence of the El Niño phenomenon,

282 experienced the highest decrease in TB in the CV simulation. In the state of Roraima, on the other hand,  
283 there was an increase of about  $2 \text{ kg-C m}^{-2}$  in TB when CV was considered. Bolivia and southwest of Mato  
284 Grosso state also presented, in some grids points, a significant increase in AGB higher than  $2 \text{ kg-C m}^{-2}$ .

285 On average, P acts as a limiting factor in the simulated TB, decreasing by 13% in regional P (PR)  
286 simulation and 15% in global P (PG) simulation. In PR, TB decreased mainly in the southeastern  
287 Amazonia (between Pará and northeastern Mato Grosso states) and northwestern Amazonas state (Figure  
288 4b). In PG, the largest TB decline occurred in central Amazonia, northeastern Pará and northeastern Mato  
289 Grosso (Figure 4c). In Cerrado, on the other hand, TB declined by 2% for PR and 9% for PG with respect  
290 to the control simulation. In PR, the few pixels in the Cerrado that have P limitation showed a significant  
291 decrease in TB (Figure 4b), while in PG the TB reduction was statistically significant for most of the  
292 Cerrado domain, except in southern Tocantins state (Figure 4c).

293 The tree biomass reduction due to fire events is much higher in magnitude more than due to P  
294 limitation or inter-annual climate variability (Figure 4d). The small or null fire effect in the Central  
295 Amazon rainforest is related the greater water availability on the Amazonia, which makes the forest  
296 naturally not flammable as well as a gradient towards seasonally dryer climate increases the intensity and  
297 magnitude of fire effects towards the Cerrado (Figure 4d). The fire effect on TB over the Amazon domain  
298 was 21-24% of the P limitation effect (range for PR and PG cases), while the fire effect on TB over the  
299 Cerrado was more than 250% of the P limitation effects in CV simulations, which is due to quick growth  
300 of grasses after fire occurrence in the latter.

### 301 **3.1.2 Influence of climate, fire and phosphorus in the transects**

302 Results of the ANOVAs and Tukey-Kramer test indicate that the inclusion of CV, limitation by P  
303 (PR and PG) and fire in INLAND led to significantly different averages of NPP, LAI and AGB in the  
304 transition zones. This influence of climate, P and fire are shown separately in Tables 3 to Table 5 and  
305 combined in Table 6.

306 The effects of climate and P on productivity show that CV reduces the NPP from  
307  $0.68 \text{ kg-C m}^{-2} \text{ yr}^{-1}$  to  $0.64 \text{ kg-C m}^{-2} \text{ yr}^{-1}$  (Table 3) and the P effect results in NPP decline from  
308  $0.71 \text{ kg-C m}^{-2} \text{ yr}^{-1}$  to  $0.64 \text{ kg-C m}^{-2} \text{ yr}^{-1}$  (both PR and PG) (Table 4). The fire effect, moreover, has a  
309 positive effect on NPP from  $0.66 \text{ kg-C m}^{-2} \text{ yr}^{-1}$  when fire is off to  $0.67 \text{ kg-C m}^{-2} \text{ yr}^{-1}$  when fires is on. This  
310 difference, albeit low, is statistically significant (Table 5).

311 In addition CV and P limitation reduce the  $\text{LAI}_{\text{total}}$  in the canopy (Table 3 and Table 4), increasing  
312 three times  $\text{LAI}_{\text{lower}}$  and decreasing  $\text{LAI}_{\text{upper}}$  (Table 5). The magnitude of fire effect on AGB (46.7%,  
313 Table 5) is greater in relation to the CV (5%, Table 3) and P (14%, Table 4) limitation effects.

314 Even though CV effects on NPP and AGB for each simulation is not statistically significant, the  
315 effects of fire and P limitation (regardless of phosphorus map) are. Fire effects are significant only for  
316 structural variables as AGB,  $\text{LAI}_{\text{total}}$ ,  $\text{LAI}_{\text{upper}}$  and  $\text{LAI}_{\text{lower}}$ . It presents an increase of LAI total of  
317  $1.52 \text{ m}^2 \text{ m}^{-2}$  in CV+PG+F in relation to CV+PG, and of  $1.32 \text{ m}^2 \text{ m}^{-2}$  in CV+PR+F in relation to CV+PR  
318 (Table 6).

### 319 **3.1.3 West-East patterns of AGB in the Amazon-Cerrado transition**

320 The model used in this study simulates > 80% of the observed AGB variability in all treatments  
321 along the transition area except in T5 (Table 7). It shows that the model is able to capture AGB variability



322 along the transition area, which is relevant when compared to studies that simulate 50% of the observed  
323 AGB variability (Senna et al., 2009; Castanho et al., 2013).

324 It is not possible to identify a treatment that best represents AGB in all transects (Table 7). A  
325 combined analysis of Table 7 and Figure 5 indicates a general agreement that observed AGB decreases  
326 from W to E in T1 to T4, and this is well captured by several configurations of the model, with specific  
327 differences among them. Overall, CA and PC configurations, being the least disturbed treatments, yield  
328 higher AGB, while the introduction of CV, PG and F reduce the AGB. However, the simulated results  
329 may be above or below the observed ones, which suggests that additional local factors are not included  
330 in the model.

331 The curves of AGB (Figure 5) show the impact of CV, PG and F along the W-E transition. PG  
332 has a high influence on the transition, decreasing the ABG especially in the western part of the transects,  
333 where the Amazon vegetation is predominant. This feature is particularly simulated in T3 and T4, where  
334 PG decrease the AGB by  $2 \text{ kg-C m}^{-2}$  in the west pixels of these transects (Figure 5). In T1, T2 and T5,  
335 AGB decline is also higher with P limitation when compared to the curves limited only by CV. However,  
336 in T1 model simulations tend to underestimate the highest and the lowest AGB extremes, and the absolute  
337 values were always underestimated, despite the improvement in correlation with the inclusion of the fire  
338 component (Table 7).

339 In T2, T3 and T4, however, fire changes the simulated AGB, making it closer to the observed  
340 AGB in the eastern pixels of the Cerrado domain (Figure 5). In T5 these relations are similar, with climate  
341 presenting less influence on AGB decrease than P, and fire appears mainly as an AGB reduction factor.

### 342 3.2 Simulated composition of vegetation

343 Most of the pixels in CA show very robust simulations, with more than 90% of the same vegetation  
344 cover in the simulated last 10 years (Figure 6a-c and 6g-i). A larger number of pixels with transitional  
345 vegetation were simulated in CV (Figure 6d-f and 6j-l). An even higher variability in CV compared  
346 to CA simulations was observed when we added the effects of P limitation and fire (Figure 6a and 6j-l).

347 The vegetation composition in all P limitation scenarios for CA simulations resulted in robust  
348 simulations for nearly all pixels, except for the north of Cerrado domain (Figures 6a, 6b and 6c). The  
349 CA+PC and CA+PR simulations had the same vegetation composition, while CA+PG replaced the  
350 deciduous forest by evergreen forest in the central Cerrado region, around 8°S 46°W (Figures 6A, 6B and  
351 6C). This behavior might be related to the higher  $P_{total}$  values in PG than PR and PC for the Cerrado region  
352 (Figure S1). Cerrado was better represented in CV+PC, CV+PR and CV+PG than in the same CA  
353 combinations (Figure 6). The occurrence of forested areas in central Cerrado decreased in CV  
354 combinations, these being replaced by the savanna or grassland vegetation class.

355 When the effect of fire was added to CA simulations, the model simulated an increase in the  
356 uncertainty on the vegetation cover classification in the Cerrado region. The effect of fire reduced the  
357 presence of deciduous forest in central Cerrado biome as well as in CA+PC, and the vegetation was  
358 replaced by evergreen forest in about 5 pixels with clay soils with large water retention capacity in  
359 CA+PC+F (Figures 6G, 6H, 6I). In this situation, where there is little water stress in the CA simulation,  
360 both evergreen and drought deciduous PFTs have each one very high LAI, and the PFT that dominates  
361 can be defined by minor effects. Fire, although active, is probably too small to be relevant in a non-  
362 stressed ecosystem. In CV simulations, however, fire effect results in the replacement of the deciduous

363 and perennial forest by savanna and grasses in all central Cerrado region (Figures 6J, 6K and 6L). These  
364 results show the limitations of CA and the importance to consider the interannual climate variability on  
365 simulations to improve the vegetation simulated.

366 For all combinations used, transitional forest areas in the northern and southwestern Cerrado  
367 biome are not adequately represented. With >90% of concordance, INLAND assigns the existence of  
368 tropical evergreen forest rather than deciduous forest in some pixels in the north of the transition, and the  
369 existence of tropical evergreen forest rather than savanna in the southwest, indicating difficulty to  
370 simulate transitional vegetation in these regions.

#### 371 **4 Discussion**

372 The inclusion of CV, PR and PG and fire in INLAND showed significant influences on the  
373 simulated vegetation structure and dynamics in the Amazon-Cerrado border (Figure 4 and Table 6),  
374 suggesting that these factors play key role on vegetation structure in the forest-savanna border and can  
375 improve the simulated representation of the current contact zone between these biomes. This is broadly  
376 consistent with the literature that investigated causes of savanna existence in the real world (Hoffmann et  
377 al., 2012; Dantas et al., 2013; Lehmann et al., 2014). In this study, the spatial analysis and the Tukey-  
378 Kramer test (TK) show a difference in magnitude among these factors in vegetation, with fire occurrence  
379 and P limitation being stronger than inter-annual climate variability along the transects (Figure 4).

380 The spatial analysis showed that CV declines AGB predominantly in eastern Amazonia (Figure  
381 4a). Climate of this region is intensely affected by ENSO, which could reduce precipitation by 50%,  
382 placing the vegetation under intense water stress (Botta and Foley, 2002; Foley et al. 2002; Marengo et  
383 al., 2004; Andreoli et al., 2012; Hilker et al., 2014). This reduction in rainfall in dry years brings in direct

384 changes in carbon flux (NPP) and stocks in leaves and wood, leading to changes in vegetation structure.  
385 In addition to inter-annual changes in the rainfall, inter-annual variability in other climate variables in CV  
386 also affect AGB, as average, maximum and minimum temperature, as well as wind speed and specific  
387 humidity, and influence photosynthesis on the model both directly (through Collatz and Farquhar  
388 equations) and indirectly (e.g. through evapotranspiration). Our results showed significant differences for  
389 most part of the biomes, except central Amazonia (Figure 4a), where CV and precipitation seasonality  
390 have been pointed as secondary effects on vegetation (Restrepo-Coupe et al., 2013), since there is no  
391 shortage of water availability during the dry season.

392         Along the Cerrado, lower water availability in some years in CV affects tree biomass, although  
393 that vegetation is predominantly grassy-herbaceous. The AGB decline is significant for most part of the  
394 simulated Cerrado domain (Figure 4a) and average values could represent half the amount of typical tree  
395 biomass in this biome. This reduction in AGB reflects INLAND's ability to simulate similar Cerrado  
396 conditions and expose the few trees to high water stress.

397         Throughout the transects, however, no significant difference was found for average AGB between  
398 CV+PC and CA+PC by TK at  $p < 0.05$  (Table 6). On the other hand, when we analyzed the influence of  
399 CV for the same pixels, but using all simulations (Table 3), regardless of P limitation and fire occurrences,  
400 the results showed that the decrease in AGB by  $0.38 \text{ kg-C m}^{-2}$  (5.7%) is statistically significant along the  
401 transition.

402         P limitation effect was statistically significant for PR and PG along all the Amazon domain and  
403 the main differences between these simulations were the spatial patterns of tree AGB decrease (Figure 4b  
404 and Figure 4c). We cannot affirm which of these databases is better because they are the results of

405 different methodologies and observations (Quesada et al., 2009; Yang et al., 2014). However, PG showed  
406 a higher AGB decrease in central Amazonia, northeastern Pará and northeastern Mato Grosso state,  
407 indicating that in these areas the P limitation is higher. This result does not corroborate the northwest-  
408 southeast AGB gradient found in the Amazon basin, which showed a higher productivity in the west  
409 where soils are more fertile than those found in the southeast (Aragão et al., 2009; Saatchi et al., 2007;  
410 Nunes et al., 2012; Lee et al., 2013). On the other hand, PR AGB agrees with the northwest-southeast  
411 gradient, presenting less limitation in the soils of central Amazonia with declines in AGB mainly in the  
412 southeastern part of the rainforest (between Pará and northeastern Mato Grosso states) (Figure 4b).

413 In Cerrado, P limitation also influenced vegetation (Figure 4c) and presented statistically  
414 significant differences when compared CV+PG – CV+PC. In this biome, as well as in the Amazon, tree  
415 abundance richness and diversity have been generally associated with increases of soil fertility (Long et  
416 al., 2012; Vourtilis et al., 2013), highlighting the importance of P in the composition and maintenance of  
417 vegetation, especially in transition areas.

418 Compared to the Amazon domain, the magnitude of effects of P limitation is lower in the Cerrado.  
419 However, few pixels in PR that have P limitation showed a significant decrease in arboreal AGB (Figure  
420 4b), while in PG, we found reduction of AGB for most of the Cerrado domain, except only for the southern  
421 Tocantins state (Figure 4c). Despite the differences in spatial patterns, there was no statistically significant  
422 differences between PR and PG within the transects (Table 4 and Table 6).

423 The spatial difference between PG and PR showed that PG is lower than PR in the western  
424 Amazonia, and higher in northern Amazonia. Moreover, PG have low P values in south of the transition  
425 compared to PR, while in Cerrado domain P values ranged between 120 to 200 mg kg<sup>-1</sup> (Figure S1).

426 Although the PR dataset includes every known P data collected in the region, these differences reinforce  
427 the need to improve the data of  $P_{total}$  in the soils of the Amazon and Cerrado/Amazon transition domains.  
428 Currently,  $P_{total}$  data in Cerrado is scarce, and make unfeasible to establish a proxy similar to Castanho et  
429 al. (2013), which was specific for the Amazon.

430 In INLAND, the simple P-limitation parameterized through the linear relation  $V_{max}$  and  $P_{total}$ ,  
431 showed significant spatial differences in AGB simulated and an improvement in simulations, highlighting  
432 the importance of P-limitation in modeling studies. For the most part, Dynamic Global Vegetation Models  
433 (DGVMs) do not consider the complete phosphorus cycle (see exceptions in Goll et al., 2012 and Yang  
434 et al., 2014), despite the importance of nutrient cycling for AGB maintenance and tropical vegetation  
435 dynamics in dystrophic soils. For example, nutrient cycling in the Amazon/Cerrado transition is closely  
436 related to the hyper-dynamic turnover of the AGB (Valadão et al. 2016), in which some key species might  
437 also be crucial to the hyper-cycling of nutrients through which vegetation sustain the constant input of  
438 nutrients, including large annual amounts of available P (Oliveira et al. 2017). In addition, there is  
439 influence between weather and nutrients: a very intense rain can leach nutrients, such as nitrogen, as well  
440 as strong winds can carry clay particles where numerous nutrients are adsorbed. However, in this work  
441 the nutritional conditions are prescribed and fixed.

442 The fire occurrence is an important factor controlling the AGB dynamics in the Cerrado or in the  
443 transition vegetation (Hoffman et al., 2003; Hoffman et al., 2012; Silvério et al., 2013; Couto-Santos et  
444 al., 2014; Balch et al., 2015), which this study clearly replicates, showing statistically significant  
445 influences when compared to control simulations (Figure 4d and Table 5). In the transition, the fire effect  
446 may reduce average AGB by 50% (Table 5), which under climate change or deforestation conditions may

447 lead to an even stronger change in the vegetation structure and dynamics. In INLAND, the fire disturbance  
448 reduces the biomass of all pools and PFT's by the same fraction inside each pixel at the end of every year.  
449 Thus, upper and lower LAI are decreased, according to the fire probability, triggering competition  
450 between both canopies for light, and increasing the photosynthesis rates and stocks of carbon in leaves,  
451 stems and roots pools in the lower canopy. The carbon allocation and mortality rates in INLAND are  
452 fixed parameters for each PFT and are not modified after fire occurrence. Thus, during recovery from a  
453 fire, the vegetation dynamics follows the model standard procedure.

454         The dynamics between the upper and lower canopies and the changes in canopy structure after  
455 fire occurrence are exclusively due to the canopy opening and consequently more penetration of  
456 photosynthetic radiation into the lower canopy. This competition implies in significant increase on the  
457 lower canopy resulting in increment of  $LAI_{lower}$  (Table 5).

458         The model does not include fire characteristics such as velocity, intensity and duration of the  
459 burning (Hoffman et al., 2003; Rezende et al., 2005; Elias et al., 2013; Reis et al., 2015) or the  
460 representation of some tree morphological adaptation that confers to Cerrado species resilience to fire  
461 occurrence, such as bark thickness. Thus, trees and grasses throughout the Amazon-Cerrado border are  
462 equally exposed to the same fire intensity inside the grid cell, without fire resistance differences.  
463 However, despite the limitations in the representation of resilience characteristics and morphological  
464 attributes of fire resistance, our results show that simulated biomass is more close to observed biomass in  
465 Cerrado areas when the fire module is activated (Figure 5). An improvement in distribution of biomes  
466 along the simulated transition area is also observed (Figure 6g-i), highlighting fire as an essential factor  
467 to represent the Amazonia-Cerrado border.

468 This study shows an improvement in the correlations between simulated and observed AGB when  
469 compared to previous modeling studies, regardless of treatment, with correlation coefficients usually  
470 above 0.80 for the transects, except for T5, for which the correlation coefficient value is usually below  
471 0.5 (Table 7). Senna et al. (2009) found 0.20 as maximum correlation coefficient between simulated and  
472 observed ABG while Castanho et al. (2013) showed 0.80 for Amazonia domain. From Figure 5, it is clear  
473 that CV, F and P limitation in the transition zone reduce the AGB, causing the simulated data to approach  
474 the observed data. However, the inclusion of these effects is still insufficient to represent the correct  
475 distribution of the vegetation types throughout the Amazon-Cerrado border (Figure 6L). In our  
476 interpretation, this means that other important factors are still missing from the simulation, especially in  
477 T5, where soils are rocky and shallow. A better spatial representation of soil physical properties, including  
478 shallow rocky soils, as well as spatially varying physiological parameterizations of the vegetation such as  
479 carbon allocation, deciduousness of vegetation, residence time, are probably needed to improve the  
480 simulations, in particular in the northern and southern extremes of the border (T1 and T5).

481 In addition, literature shows that in the transition area, soils are very different than Amazon soils,  
482 and that essential proprieties for modeling are peculiar (Silva et al., 2006; Vourlitis et al., 2013; Dias et  
483 al. 2015). For example, Dias et al. (2015) recently showed that the pedological functions normally used  
484 by DGVMs may underestimate the saturated hydraulic conductivity ( $K_s$ ) by >99%, transforming a well-  
485 drained soil with  $K_s = 1.5 \cdot 10^{-4} \text{ m.s}^{-1}$  (540  $\text{mm.h}^{-1}$ ) in reality into an impervious brick with  
486  $K_s = 3.3 \cdot 10^{-7} \text{ m.s}^{-1}$  (1.2  $\text{mm.h}^{-1}$ ) in the model.

487 For all transects, the AGB curves have similar patterns (Figure 5); the smaller difference is  
488 observed between CA+PC and CV+PG curves, while the larger difference is when fire is present. The



489 effect of P limitation appears as an effect of intermediate magnitude, reducing the AGB by more than the  
490 effect of inter-annual climate variability. In the east, it is observed that there is little or no difference  
491 among AGB simulated by CA+PC, CV+PC and CV+PG, revealing that inter-annual climate variability  
492 and P have smaller influence in the AGB. However, in the east of T2, T3 and T4, fire is the factor that  
493 adjusts the simulated to the observed data (Figure 5), differently than the grid points in the West, where  
494 CV+PG is a better proxy between observed and simulated data.

495         Such conditions are interesting because they reflect the different mechanisms that regulate the  
496 structure of these ecosystems and probably the phytophysiognomies distribution. For example, P  
497 limitation seems to be the factor that improves simulated AGB in regions where the predominant  
498 vegetation type is the tropical rainforest. Fire, on the other hand, improves the AGB in grid points where  
499 the Cerrado occurs. Moreover, important factors such as productivity partitioning into leaves, roots and  
500 wood carbon pools are assumed to be fixed in space and time within a given PFT, neglecting the natural  
501 capacity of transitional forests to adapt itself and to adjust their metabolism to local environmental  
502 conditions (Senna et al., 2009). In years of severe drought, or under frequent fire occurrence, transitional  
503 forests could prioritize the stock of carbon in fine roots instead of the basal or leaf increment to maximize  
504 access to available water, make hydraulic redistribution of soil moisture to maintain the greenness and  
505 photosynthesis rates, or increase the capacity to resprout after fire occurrence (Hoffman et al., 2003;  
506 Brando et al., 2008). Brando et al. (2008) found changes in carbon allocation after an artificial drought in  
507 eastern Amazonia, with wood production reduced by 13-60%, and associated increase in root production.  
508 Although in INLAND low soil moisture can reduce the photosynthetic rates, carbon allocation rates are  
509 fixed (Figure 5a).

510 T2, T3 and T4, located in the central part of the Amazon-Cerrado transition, showed the highest  
511 average correlations between observed and simulated data (Table 7). For these transects, INLAND seems  
512 to be able to capture the high variability of AGB gradient.

513 At T5, located at the south of the transition, the average correlations were low for all treatments,  
514 indicating that INLAND has difficulty to represent the AGB gradient there (Table 7). However, it captures  
515 the lower AGB as compared to the northern ones. In this region, the vegetation is characterized by a wide  
516 diversity of physiognomies, which varies with other preponderant factors, such as lithology, soil depth,  
517 topography and fertility. The observed data also showed high AGB variability, indicating that there are  
518 changes in the vegetation structure, featuring medium-sized and small vegetation types on different soil  
519 types. In INLAND, however, features such as lithology and water-table depth are not considered due to  
520 the complexity of its representation on the large scale, limiting the representation of a heterogeneous  
521 environment throughout the transition.

522 Patterns of vegetation distribution along the Amazon-Cerrado border exist are influenced not only  
523 by inter-annual climate variability, P limitation, and fire, but also by the ecophysiological parameters.  
524 Additional field experiments are needed to understand the relationship between currently fixed parameters  
525 (such as carbon allocation, residence time, and deciduousness, among others) to the environmental  
526 conditions and soil proprieties.

527 Another point to discuss is that the model simulates, in a few pixels in southeastern Cerrado, very  
528 robust simulations of the presence of savanna and grassland even in the absence of fire (Figure 6A-F and  
529 6a-f). This is, in our view, a result of the intense water and heat stress in this region. In the Brazilian  
530 Cerrado, the high temperatures ( $> 35\text{ }^{\circ}\text{C}$ ) combined to the dry season duration (as long as 6 months with

531 little or no rain) exposes the vegetation to a severely stressed situation, so that a low biomass, low LAI  
532 vegetation may exist without the need of a frequent disturbance.

533

## 534 **5 Conclusions**

535 This is the first study that uses modeling to assess the influence of inter-annual climate variability,  
536 fire occurrence and phosphorus limitation to represent the Amazon-Cerrado border. This study shows  
537 that, although the model forced by a climatological database is able to simulate basic characteristics of  
538 the Amazon-Cerrado transition, the addition of factors such as inter-annual climate variability,  
539 phosphorus limitation and fire gradually improves simulated vegetation types. These effects are not  
540 homogeneous along the latitudinal/longitudinal gradient, which makes the adequate simulation of  
541 biomass challenging in some places along the transition. Based on the F-statistic in Tables 3, 4 and 5, this  
542 work shows that fire is in the main determinant factor of the changes in vegetation structure (LAI, AGB)  
543 along the transition. The nutrient limitation is second in magnitude, stronger than the effect of inter-annual  
544 climate variability.

545 Overall, although INLAND typically simulates more than 80% of the variability of biomass in the  
546 transition zone, in many places the biomass is clearly not well simulated. Situations for clearly wet or  
547 markedly dry climate conditions were well simulated, but the simulations are generally poor for  
548 transitional areas where the environment selected physiognomies that have an intermediate behavior, as  
549 is the case of the transitional forests in northern Tocantins and Mato Grosso.

550 There is evidence that the inclusion of spatially explicit parameters such as woody biomass  
551 residence time, maximum carboxylation capacity ( $V_{\max}$ ), and NPP allocation to wood may improve

552 Amazon rainforest AGB simulation by DGVMs (Castanho et al., 2013). However, in the transition, the  
553 lack of field parameters measured limits the inclusion of the variability of these biophysical parameters  
554 in DGVMs. Additional field work and compilation of existing ones are necessary to obtain physiological  
555 and structural parameters through the Amazon-Cerrado border to establish numerical relationships  
556 between soil, climate and vegetation. With the help of these data, dynamic vegetation models will be able  
557 to improve simulation of current patterns and future changes in vegetation considering climate change  
558 scenarios. In addition, it is also needed to include not only the spatial variability, but also temporal  
559 variability in physiological parameters of vegetation, allowing a more realistic simulation of the  
560 soil-climate-vegetation relationship. Finally, our results reinforce the importance and need of the DGVMs  
561 to incorporate the nutrient limitation and fire occurrence to simulate the Amazon-Cerrado border position.

562

## 563 **6 Acknowledgements**

564 We gratefully thank the Brazilian agencies FAPEMIG and CAPES for their financial support. Atul  
565 K Jain is funded by the U.S. National Science Foundation (NSF-AGS- 12-43071).

## 566 **7 References**

567 Andreoli, R. V., Ferreira de Souza, R. A., Kayano, M. T. and Candido, L. A.: Seasonal anomalous  
568 rainfall in the central and eastern Amazon and associated anomalous oceanic and atmospheric patterns,  
569 *Int. J. Climatol.*, 32(8), 1193–1205, doi:10.1002/joc.2345, 2012.

570 Aragão, L. E. O. C., Malhi, Y., Metcalfe, D. B., Silva-Espejo, J. E., Jiménez, E., Navarrete, D.,  
571 Almeida, S., Costa, A. C. L., Salinas, N., Phillips, O. L., Anderson, L. O., Baker, T. R., Goncalvez, P. H.,  
572 Huamán-Ovalle, J., Mamani-Solórzano, M., Meir, P., Monteagudo, A., Peñuela, M. C., Prieto, A.,

573 Quesada, C. A., Rozas-Dávila, A., Rudas, A., Silva Junior, J. A. and Vásquez, R.: Above- and below-  
574 ground net primary productivity across ten Amazonian forests on contrasting soils, *Biogeosciences*, 6,  
575 2441–2488, doi:10.5194/bgd-6-2441-2009, 2009.

576 Arora, V. K. and Boer, G. J.: Fire as an interactive component of dynamic vegetation models, *J.*  
577 *Geophys. Res.*, 110, doi:10.1029/2005JG000042, 2005

578 Balch, J. K., Brando, P. M., Nepstad, D. C., Coe, M. T., Silvério, D., Massad, T. J., Davidson, E.  
579 A., Lefebvre, P., Oliveira-Santos, C., Rocha, W., Cury, R. T. S., Parsons, A. and Carvalho, K. S.: The  
580 Susceptibility of Southeastern Amazon Forests to Fire: Insights from a Large-Scale Burn Experiment,  
581 *Bioscience*, 65(9), 893–905, doi:10.1093/biosci/biv106, 2015.

582 Beguería, S., Vicente-Serrano, S. M., Tomás-Burguera, M. and Maneta, M.: Bias in the variance  
583 of gridded data sets leads to misleading conclusions about changes in climate variability. *Int. J. Climatol.*,  
584 36: 3413–3422. doi:10.1002/joc.4561, 2016.

585 Betts, R. A., Cox, P. M., Collins, M., Harris, P. P., Huntingford, C. and Jones, C. D.: The role of  
586 ecosystem-atmosphere interactions in simulated Amazonian precipitation decrease and forest dieback  
587 under global climate warming, *Theor. Appl. Climatol.*, 78, 157–175, doi:10.1007/s00704-004-0050-y,  
588 2004.

589 Bonan, G. B.: Forests and climate change: forcings, feedbacks, and the climate benefits of forests,  
590 *Science*, 320(5882), 1444–1449, doi:10.1126/science.1155121, 2008.

591 Bond, W. J., Woodward, F. I. and Midgley, G. F.: The global distribution of ecosystems in a world  
592 without fire, *New Phytol.*, 165(2), 525–538, doi:10.1111/j.1469-8137.2004.01252.x, 2005.

593 Botta, A. and Foley, J. A.: Effects of climate variability and disturbances on the Amazonian  
594 terrestrial ecosystems dynamics, *Global Biogeochem. Cycles*, 16(4), doi:10.1029/2000GB001338, 2002.

595 Brando, P. M., Nepstad, D. C., Davidson, E. A., Trumbore, S. E., Ray, D. and Camargo, P.:  
596 Drought effects on litterfall, wood production and belowground carbon cycling in an Amazon forest:  
597 results of a throughfall reduction experiment, *Philos. Trans. R. Soc. Lond. B. Biol. Sci.*, 363(1498), 1839–  
598 48, doi:10.1098/rstb.2007.0031, 2008.

599 Castanho, A. D. A., Coe, M. T., Costa, M. H., Malhi, Y., Galbraith, D. and Quesada, C. A.:  
600 Improving simulated Amazon forest AGB and productivity by including spatial variation in biophysical  
601 parameters, *Biogeosciences*, 10(4), 2255–2272, doi:10.5194/bg-10-2255-2013, 2013.

602 Couto-Santos, F. R., Luizão, F. J. and Carneiro Filho, A.: The influence of the conservation status  
603 and changes in the rainfall regime on forest-savanna mosaic dynamics in Northern Brazilian Amazonia,  
604 *Acta Amaz.*, 44(2), 197–206, 2014.

605 Cox, P. M., Betts, R. A., Jones, C. D., Spall, S. A. and Totterdell, I. J.: Acceleration of global  
606 warming due to carbon-cycle feedbacks in a coupled climate model, *Nature*, 408(November), 184–187,  
607 doi:10.1038/35041539, 2000.

608 Cox, P. M., Betts, R. A., Collins, M., Harris, P. P., Huntingford, C. and Jones, C. D.: Amazonian  
609 forest dieback under climate-carbon cycle projections for the 21st century, *Theor. Appl. Climatol.*, 78,  
610 137–156, doi:10.1007/s00704-004-0049-4, 2004.

611 Dajoz, R.: *Princípios de ecologia*, 7<sup>o</sup> edição, Artmed, Porto Alegre, RS, Brazil 519pp, 2005.

612 Dantas, V. L., Batalha, M. A. and Pausas, J. G.: Fire drives functional thresholds on the savanna-  
613 forest transition, *Ecology*, 94(11), 2454–2463, doi:10.1890/12-1629.1, 2013.

614 Davidson, E. A., Carvalho, C. J.R., Vieira, I. C. G., Figueiredo, R. D. O., Moutinho, P., Ishida,  
615 F.Y., Santos, M. T.P., Guerrero, J.B., Kalif, K. and Sabá, R.T.: Nitrogen and Phosphorus Limitation of  
616 Biomass Growth in a Tropical Secondary Forest, *Ecol. Appl.*, 14(4), 150–163, doi:10.1890/01-6006,  
617 2004.

618 Dias, L. C. P., Macedo, M. N., Costa, M. H., Coe, M. T. and Neill, C.: Effects of land cover change  
619 on evapotranspiration and streamflow of small catchments in the Upper Xingu River Basin, Central  
620 Brazil, *J. Hydrol. Reg. Stud.*, 4, 108–122, doi:10.1016/j.ejrh.2015.05.010, 2015.

621 Elias, F., Marimon, B. S., Matias, S. R. A., Forsthofer, M., Morandi, P. S. and Marimon-junior,  
622 B. H.: Dinâmica da distribuição espacial de populações arbóreas, ao longo de uma década, em cerrado  
623 na transição Cerrado-Amazônia, *Mato Grosso, Biota Amaz.*, 3, 1–14, 2013.

624 Favier, C., Chave, J., Fabing, A., Schwartz, D. and Dubois, M. A.: Modelling forest-savanna  
625 mosaic dynamics in man-influenced environments: Effects of fire, climate and soil heterogeneity, *Ecol.*  
626 *Modell.*, 171, 85–102, doi:10.1016/j.ecolmodel.2003.07.003, 2004.

627 Foley, J. A., Prentice, I. C., Ramankutty, N., Levis, S., Pollard, D., Sitch, S. and Haxeltine, A.: An  
628 integrated biosphere model of land surface processes, terrestrial carbon balance, and vegetation dynamics,  
629 *Global Biogeochem. Cycles*, 10, 603, doi:10.1029/96GB02692, 1996.

630 Foley, J. A., Botta, A., Coe, M. T. and Costa, M. H.: El Niño–Southern oscillation and the  
631 climate, ecosystems and rivers of Amazonia, *Global Biogeochem. Cycles*, 16(4), 1132,  
632 doi:10.1029/2002GB001872, 2002.

633 Goedert, W: Solos do Cerrado: Tecnologias e Estratégias de Manejo, Empresa Brasileira de  
634 Pesquisa Agropecuária (EMBRAPA), Brasília, DF, Brasil. 422pp., 1986.

635 Goll, D. S., V. Brovkin, B. R. Parida, C. H. Reick, J. Kattge, P. B. Reich, P. M. Van Bodegom,  
636 and Ü. Niinemets.: Nutrient limitation reduces land carbon uptake in simulations with a model of  
637 combined carbon, nitrogen and phosphorus cycling, *Biogeosciences*, 9(C), 3547–3569, doi:10.5194/bg-  
638 9-3547-2012,2012.

639 Hansen, M. C. and Reed, B.: A comparison of the IGBP DISCover and University of Maryland  
640 1km global land cover products, *Int. J. Remote Sens.*, 21, 1365–1373, doi:10.1080/014311600210218,  
641 2000.

642 Harris, I., Jones, P. D., Osborn, T. J. and Lister, D. H.: Updated high-resolution grids of monthly  
643 climatic observations - the CRU TS3.10 Dataset, *Int. J. Climatol.*, 34(3), 623–642, doi:10.1002/joc.3711,  
644 2014.

645 Hilker, T., Lyapustin, A. I., Tucker, C. J., Hall, F. G., Myneni, R. B., Wang, Y., Bi, J., Mendes de  
646 Moura, Y. and Sellers, P. J.: Vegetation dynamics and rainfall sensitivity of the Amazon., *Proc. Natl.*  
647 *Acad. Sci. U. S. A.*, 111(45), 16041–6, doi:10.1073/pnas.1404870111, 2014.

648 Hirota, M., Nobre, C., Oyama, M. D. and Bustamante, M. M. C.: The climatic sensitivity of the  
649 forest, savanna and forest-savanna transition in tropical South America, *New Phytol.*, 187, 707–719,  
650 doi:10.1111/j.1469-8137.2010.03352.x, 2010.

651 Hoffmann, W. A., B. Orthen, and P. K. V. Nascimento.: Comparative fire ecology of tropical  
652 savanna and forest trees, *Functional Ecology*, 17:720–726, 2003.

653 Hoffmann, W.A., Adasme, R., Haridasan, M., Carvalho, M., Geiger, E.L., Pereira, M.A.B.,  
654 Gotsch, S.G., and Franco, A.C.: Tree topkill, not mortality, governs the dynamics of alternate stable states  
655 at savanna-forest boundaries under frequent fire in central Brazil, *Ecology*, 90, 1326–1337, 2009.



656 Hoffmann, W. A., Geiger, E. L., Gotsch, S. G., Rossatto, D. R., Silva, L. C. R., Lau, O. L.,  
657 Haridasan, M. and Franco, A. C.: Ecological thresholds at the savanna-forest boundary: How plant traits,  
658 resources and fire govern the distribution of tropical biomes, *Ecol. Lett.*, 15, 759–768,  
659 doi:10.1111/j.1461-0248.2012.01789.x, 2012.

660 House, J. I., Archer, S., Breshears, D. D. and Scholes, R. J.: Conundrums in mixed woody-  
661 herbaceous plant systems, *J. Biogeogr.*, 30, 1763–1777, doi:10.1046/j.1365-2699.2003.00873.x, 2003.

662 IBGE.: Manual Técnico da Vegetação Brasileira (Manuais Técnicos em Geociências n. 1),  
663 Fundação Instituto Brasileiro de Geografia e Estatística (IBGE), Rio de Janeiro, RJ, Brasil. 92pp., 1992.

664 IBGE.: Mapa da Vegetação do Brasil, Fundação Instituto Brasileiro de Geografia e Estatística  
665 (IBGE), Rio de Janeiro, RJ, Brazil, Map, 2004.

666 Klink, C. A. and Machado, R. B.: Conservation of the Brazilian Cerrado, *Conserv. Biol.*, 19(3),  
667 707–713, doi:10.1111/j.1523-1739.2005.00702.x, 2005.

668 Kucharik, C. J., Foley, J. A., Delire, C., Fisher, V. A., Coe, M. T., Lenters, J. D., Young-Molling,  
669 C., Ramankutty, N., Norman, J. M. and Gower, S. T.: Testing the performance of a Dynamic Global  
670 Ecosystem Model: Water balance, carbon balance, and vegetation structure, *Global Biogeochem. Cycles*,  
671 14(3), 795–825, doi:10.1029/1999GB001138, 2000.

672 Lee, J. E., Frankenberg, C., van der Tol, C., Berry, J. A., Guanter, L., Boyce, C. K., Fisher, J. B.,  
673 Morrow, E., Worden, J. R., Asefi, S., Badgley, G. and Saatchi, S.: Forest productivity and water stress in  
674 Amazonia: observations from GOSAT chlorophyll fluorescence, *Proc. R. Soc. B Biol. Sci.*, 280(1761),  
675 20130171–20130171, doi:10.1098/rspb.2013.0171, 2013.

676 Lehmann, C. E. R., Archibald, S. A., Hoffmann, W. A. and Bond, W. J.: Deciphering the  
677 distribution of the savanna biome, *New Phytol.*, 191, 197–209, doi:10.1111/j.1469-8137.2011.03689.x,  
678 2011.

679 Lehmann, C. E. R., Anderson, T. M., Sankaran, M., Higgins, S. I., Archibald, S., Hoffmann, W.  
680 A., Hanan, N. P., Williams, R. J., Fensham, R. J., Felfili, J., Hutley, L. B., Ratnam, J., Jose, J. S., Montes,  
681 R., Franklin, D., Russell-Smith, J., Ryan, C. M., Durigan, G., Hiernaux, P., Haidar, R., Bowman, D. M.  
682 J. S., and Bond, W. J.: Savanna Vegetation-Fire-Climate Relationships Differ Among Continents,  
683 *Science*, 343 (January), 548–553, doi:10.1126/science.1247355, 2014.

684 Long, W., Yang, X. and Donghai, L.: Patterns of species diversity and soil nutrients along a  
685 chronosequence of vegetation recovery in Hainan Island, South China, *Ecol. Res.*, 2012.

686 Malhi, Y., Aragão, L. E. O. C., Metcalfe, D. B., Paiva, R., Quesada, C. A., Almeida, S., Anderson,  
687 L., Brando, P., Chambers, J. Q., da Costa, A. C. L., Hutyra, L. R., Oliveira, P., Patiño, S., Pyle, E. H.,  
688 Robertson, A. L. and Teixeira, L. M.: Comprehensive assessment of carbon productivity, allocation and  
689 storage in three Amazonian forests, *Glob. Chang. Biol.*, 15, 1255–1274, doi:10.1111/j.1365-  
690 2486.2008.01780.x, 2009.

691 Marengo, J. A.: Interdecadal variability and trends of rainfall across the Amazon basin, *Theor.*  
692 *Appl. Climatol.*, 78(1–3), 79–96, doi:10.1007/s00704-004-0045-8, 2004.

693 Marimon Junior, B. H. and Haridasan, M.: Comparação da vegetação arbórea e características  
694 edáficas de um cerradão e um cerrado sensu stricto em áreas adjacentes sobre solo distrófico no leste de  
695 Mato Grosso, Brasil, *Acta Bot. Brasilica*, 19(4), 913–926, doi:10.1590/S0102-33062005000400026,  
696 2005.

697 Marimon, B. S., Lima, E. S., Duarte, T. G., Chieregatto, L. C., Ratter, J. A.: Observations on the  
698 vegetation of northeastern Mato Grosso, Brazil. IV. An analysis of the Cerrado-Amazonian Forest  
699 ecotone, *Edinburgh Journal of Botany*, 63, 323–341, doi: 10.1017/S0960428606000576, 2006.

700 Marimon, B. S., Marimon-Junior, B. H., Feldpausch, T. R., Oliveira-Santos, C., Mews, H. A.,  
701 Lopez-Gonzalez, G., Lloyd, J., Franczak, D. D., de Oliveira, E. A., Maracahipes, L., Miguel, A., Lenza,  
702 E. and Phillips, O. L.: Disequilibrium and hyperdynamic tree turnover at the forest–cerrado transition  
703 zone in southern Amazonia, *Plant Ecol. Divers.*, 7(1–2), 281–292, doi:10.1080/17550874.2013.818072,  
704 2014.

705 Mercado, L. M., Patino, S., Domingues, T. F., Fyllas, N. M., Weedon, G. P., Sitch, S., Quesada,  
706 C. A., Phillips, O. L., Aragao, L. E. O. C., Malhi, Y., Dolman, A. J., Restrepo-Coupe, N., Saleska, S. R.,  
707 Baker, T. R., Almeida, S., Higuchi, N. and Lloyd, J.: Variations in Amazon forest productivity correlated  
708 with foliar nutrients and modelled rates of photosynthetic carbon supply, *Philos. Trans. R. Soc. Lond. B.*  
709 *Biol. Sci.*, 366(1582), 3316–3329, doi:10.1098/rstb.2011.0045, 2011.

710 Morandi, P.S., Marimon-Junior, B. H., Oliveira, E. A., Reis, S. M. A., Valadão, M. B. X.,  
711 Forsthofer, M., Passos, F. B., Marimon, B. S.: Vegetation Succession in the Cerrado-Amazonian Forest  
712 Transition Zone of Mato Gross State, Brazil, *Edinburgh Journal of Botany*, 73, 83-93, doi:  
713 10.1017/S096042861500027X, 2016.

714 Moreno, M. I. C., Schiavini, I. and Haridasan, M.: Fatores edáficos influenciando na estrutura de  
715 fitofisionomias do cerrado, *Caminhos da Geogr.*, 9(25), 173–194, 2008.

716 Murphy, B. P. and Bowman, D. M. J. S.: What controls the distribution of tropical forest and  
717 savanna?, *Ecol. Lett.*, 15, 748–758, doi:10.1111/j.1461-0248.2012.01771.x, 2012.

718 Myers, N., Fonseca, G. A. B., Mittermeier, R. A., Fonseca, G. A. B. and Kent, J.: Biodiversity  
719 hotspots for conservation priorities, *Nature*, 403(6772), 853–858, doi:10.1038/35002501, 2000.

720 Nardoto, G. B., Bustamante, M. M. C., Pinto, A. S. and Klink, C. A. Nutrient use efficiency at  
721 ecosystem and species level in savanna areas of Central Brazil and impacts of fire, *J. Trop. Ecol.*, 22,  
722 191–201, doi:10.1017/S0266467405002865, 2006.

723 Nogueira, E. M., Yanai, A. M., Fonseca, F. O. and Fearnside, P. M.: Carbon stock loss from  
724 deforestation through 2013 in Brazilian Amazonia, *Glob. Chang. Biol.*, doi:10.1111/gcb.12798, 2015.

725 Nunes, E. L., Costa, M. H., Malhado, A. C. M., Dias, L. C. P., Vieira, S. A., Pinto, L. B. and Ladle,  
726 R. J.: Monitoring carbon assimilation in South America’s tropical forests: Model specification and  
727 application to the Amazonian droughts of 2005 and 2010, *Remote Sens. Environ.*, 117, 449–463,  
728 doi:10.1016/j.rse.2011.10.022, 2012.

729 Oliveira, B., Marimon-Junior, B. H., Mews, H. A., Valadão, M. B. X., Marimon, B. S.: Unraveling  
730 the ecosystem functions in the Amazonia–Cerrado transition: evidence of hyperdynamic nutrient cycling,  
731 *Plant Ecol.*, 218(2), 225–239, doi:10.1007/s11258-016-0681-y, 2017.

732 Oyama, M. D. and Nobre, C. A.: A new climate-vegetation equilibrium state for Tropical South  
733 America, *Geophys. Res. Lett.*, 30(23), 10–13, doi:10.1029/2003GL018600, 2003.

734 Parton, W. J., Scurlock, J. M. O., Ojima, D. S., Gilmanov, T. G., Scholes, R. J., Schimel, D. S.,  
735 Kirchner, T., Menaut, J.-C., Seastedt, T., Garcia Moya, E., Kamnalrut, A. and Kinyamario, J. I.:  
736 Observations and modeling of AGB and soil organic matter dynamics for the grassland biome worldwide,  
737 *Global Biogeochem. Cycles*, 7, 785, doi:10.1029/93GB02042, 1993.

738 Pereira, M. P. S., Malhado, A. C. M. and Costa, M. H.: Predicting land cover changes in the  
739 Amazon rainforest: An ocean-atmosphere-biosphere problem, *Geophys. Res. Lett.*, 39(9),  
740 doi:10.1029/2012GL051556, 2012.

741 Pires, G. F. and Costa, M. H.: Deforestation causes different subregional effects on the Amazon  
742 bioclimatic equilibrium, *Geophys. Res. Lett.*, 40(14), 3618–3623, doi:10.1002/grl.50570, 2013.

743 Quesada, C. A., Lloyd, J., Schwarz, M., Baker, T. R., Phillips, O. L., Patiño, S., Czimczik, C.,  
744 Hodnett, M. G., Herrera, R., Arneeth, A., Lloyd, G., Malhi, Y., Dezzee, N., Luizão, F. J., Santos, A. J. B.,  
745 Schmerler, J., Arroyo, L., Silveira, M., Priante Filho, N., Jimenez, E. M., Paiva, R., Vieira, I., Neill, D.  
746 A., Silva, N., Peñuela, M. C., Monteagudo, A., Vásquez, R., Prieto, A., Rudas, A., Almeida, S., Higuchi,  
747 N., Lezama, A. T., López-González, G., Peacock, J., Fyllas, N. M., Alvarez Dávila, E., Erwin, T., di Fiore,  
748 A., Chao, K. J., Honorio, E., Killeen, T., Peña Cruz, A., Pitman, N., Núñez Vargas, P., Salomão, R.,  
749 Terborgh, J. and Ramírez, H.: Regional and large-scale patterns in Amazon forest structure and function  
750 are mediated by variations in soil physical and chemical properties, *Biogeosciences Discuss.*, 6, 3993–  
751 4057, doi:10.5194/bgd-6-3993-2009, 2009.

752 Quesada, C. A., Lloyd, J., Anderson, L. O., Fyllas, N. M., Schwarz, M. and Czimczik, C. I.: Soils  
753 of Amazonia with particular reference to the RAINFOR sites, *Biogeosciences*, 8, 1415–1440,  
754 doi:10.5194/bg-8-1415-2011, 2011.

755 Quesada, C. A., Phillips, O. L., Schwarz, M., Czimczik, C. I., Baker, T. R., Patiño, S., Fyllas, N.  
756 M., Hodnett, M. G., Herrera, R., Almeida, S., Alvarez Dávila, E., Arneeth, A., Arroyo, L., Chao, K. J.,  
757 Dezzee, N., Erwin, T., Di Fiore, A., Higuchi, N., Honorio Coronado, E., Jimenez, E. M., Killeen, T.,  
758 Lezama, A. T., Lloyd, G., López-González, G., Luizão, F. J., Malhi, Y., Monteagudo, A., Neill, D. A.,

759 Núñez Vargas, P., Paiva, R., Peacock, J., Peñuela, M. C., Peña Cruz, A., Pitman, N., Priante Filho, N.,  
760 Prieto, A., Ramírez, H., Rudas, A., Salomão, R., Santos, A. J. B., Schmerler, J., Silva, N., Silveira, M.,  
761 Vásquez, R., Vieira, I., Terborgh, J. and Lloyd, J.: Basin-wide variations in Amazon forest structure and  
762 function are mediated by both soils and climate, *Biogeosciences*, 9(6), 2203–2246, doi:10.5194/bg-9-  
763 2203-2012, 2012.

764 Reis, S. M., Marimon, B. S., Marimon Junior, B.-H., Gomes, L., Morandi, P. S., Freire, E. G. and  
765 Lenza, E.: Resilience of savanna forest after clear-cutting in the Cerrado-Amazon transition zone,  
766 *Bioscience*, 31(5), 1519–1529, doi:10.14393/BJ-v31n5a2015-26368, 2015.

767 Restrepo-Coupe, N., da Rocha, H. R., Hutyra, L. R., da Araujo, A. C., Borma, L. S.,  
768 Christoffersen, B., Cabral, O. M. R., de Camargo, P. B., Cardoso, F. L., da Costa, A. C. L., Fitzjarrald,  
769 D. R., Goulden, M. L., Kruijt, B., Maia, J. M. F., Malhi, Y. S., Manzi, A. O., Miller, S. D., Nobre, A. D.,  
770 von Randow, C., S, L. D. A., Sakai, R. K., Tota, J., Wofsy, S. C., Zanchi, F. B. and Saleska, S. R.: What  
771 drives the seasonality of photosynthesis across the Amazon basin? A cross-site analysis of eddy flux tower  
772 measurements from the Brazil flux network, *Agric. For. Meteorol.*, 182–183, 128–144,  
773 doi:10.1016/j.agrformet.2013.04.031, 2013.

774 Rezende, A. V, Sanquetta, C. R. and Filho, F. A.: Efeito do desmatamento no estabelecimento de  
775 espécies lenhosas em um cerrado *Sensu stricto*, *Floresta*, 35, 69–88, 2005.

776 Ribeiro, J. F. and Walter, B. M. T.: As Principais Fitofisionomias do bioma Cerrado, in *Cerrado:*  
777 *ecologia e flora*, pp. 153–212., 2008.

778 Rocha, H. R. da, Goulden, M. L., Miller, S. D., Menton, M. C., Pinto, L. D. V. O., De Freitas, H.  
779 C. and Figueira, A. M. E. S.: Seasonality of water and heat fluxes over a tropical forest in eastern  
780 Amazonia, *Ecol. Appl.*, 14(4 SUPPL.), doi:10.1890/02-6001, 2004.

781 Roy, S. B. and Avissar, R.: Impact of land use/land cover change on regional hydrometeorology  
782 in Amazonia, *J. Geophys. Res.*, 107(D20), 1–12, doi:10.1029/2000JD000266, 2002.

783 Saatchi, S., Houghton, R. A., Dos Santos Alvalá, R. C., Soares, J. V. and Yu, Y.: Distribution of  
784 aboveground live AGB in the Amazon basin, *Glob. Chang. Biol.*, 13(4), 816–837, doi:10.1111/j.1365-  
785 2486.2007.01323.x, 2007.

786 Salazar, L. F., Nobre, C. A. and Oyama, M. D.: Climate change consequences on the biome  
787 distribution in tropical South America, *Geophys. Res. Lett.*, 34(April), 2–7, doi:10.1029/2007GL029695,  
788 2007.

789 Senna, M. C. A., Costa, M. H., Pinto, L. I.C., Imbuzeiro, H. M. A., Diniz, L. M. F. and Pires, G.  
790 F.: Challenges to reproduce vegetation structure and dynamics in Amazonia using a coupled climate-  
791 biosphere model, *Earth Interact.*, 13(11), doi:10.1175/2009EI281.1, 2009.

792 Shukla, J., Nobre, C. and Sellers, P.: Amazon deforestation and climate change, *Science*, 247,  
793 1322–1325, doi:10.1126/science.247.4948.1322, 1990.

794 Silva, J. F., Fariñas, M. R., Felfili, J. M. and Klink, C. A.: Spatial heterogeneity, land use and  
795 conservation in the cerrado region of Brazil, in *Journal of Biogeography*, vol. 33, pp. 536–548., 2006.

796 Silvério, D. V, Brando, P. M., Balch, J. K., Putz, F. E., Nepstad, D. C., Oliveira-Santos, C. and  
797 Bustamante, M. M. C.: Testing the Amazon savannization hypothesis: fire effects on invasion of a

798 neotropical forest by native cerrado and exotic pasture grasses, *Philos. Trans. R. Soc. Lond. B. Biol. Sci.*,  
799 368, 20120427, doi:10.1098/rstb.2012.0427, 2013.

800 Smith, B., Wärlind, D., Arneth, A., Hickler, T., Leadley, P., Siltberg, J. and Zaehle, S.:  
801 Implications of incorporating N cycling and N limitations on primary production in an individual-based  
802 dynamic vegetation model, *Biogeosciences*, 11(7), 2027–2054, doi:10.5194/bg-11-2027-2014, 2014.

803 Thompson, S. L. and Pollard, D.: A global climate model (GENESIS) with a land-surface transfer  
804 scheme (LSX). Part I: present climate simulation, *J. Clim.*, 8, 732–761, doi:10.1175/1520-  
805 0442(1995)008<0732:AGCMWA>2.0.CO;2, 1995.

806 Torello-Raventos, M., Feldpausch, T., Veenendaal, E., Schrodte, F., Saiz, G., Domingues, T.,  
807 Djangbletey, G., Ford, A., Kemp, J., Marimon, B., Hur Marimon Junior, B., Lenza, E., Ratter, J.,  
808 Maracahipes, L., Sasaki, D., Sonké, B., Zapfack, L., Taedoumg, H., Villarroel, D., Schwarz, M., Quesada,  
809 C., Yoko Ishida, F., Nardoto, G., Affum-Baffoe, K., Arroyo, L., Bowman, D., Compaore, H., Davies, K.,  
810 Diallo, A., Fyllas, N., Gilpin, M., Hien, F., Johnson, M., Killeen, T., Metcalfe, D., Miranda, H., Steininger,  
811 M., Thomson, J., Sykora, K., Mougín, E., Hiernaux, P., Bird, M., Grace, J., Lewis, S., Phillips, O. and  
812 Lloyd, J.: On the delineation of tropical vegetation types with an emphasis on forest/savanna transitions,  
813 *Plant Ecol. Divers.*, 6, 101–137, doi:10.1080/17550874.2012.76281, 2013.

814 Valadão, M. B. X., Marimon-Junior, B. H., Oliveira, B., Lúcio, N. W., Souza, M. G. R., Marimon,  
815 B. S.: AGB hyperdynamic as a key modulator of forest self-maintenance in dystrophic soil at Amazonia-  
816 Cerrado transition. *Scientia Forestalis*, 44, 475-485, 2016.

817 Veenendaal, E. M., Torello-Raventos, M., Feldpausch, T. R., Domingues, T. F., Gerard, F.,  
818 Schrodte, F., Saiz, G., Quesada, C. A., Djangbletey, G., Ford, A., Kemp, J., Marimon, B. S., Marimon-



819 Junior, B. H., Lenza, E., Ratter, J. A., Maracahipes, L., Sasaki, D., Sonk, B., Zapfack, L., Villarroel, D.,  
820 Schwarz, M., Yoko Ishida, F., Gilpin, M., Nardoto, G. B., Affum-Baffoe, K., Arroyo, L., Bloomfield, K.,  
821 Ceca, G., Compaore, H., Davies, K., Diallo, A., Fyllas, N. M., Gignoux, J., Hien, F., Johnson, M., Mougín,  
822 E., Hiernaux, P., Killeen, T., Metcalfe, D., Miranda, H. S., Steininger, M., Sykora, K., Bird, M. I., Grace,  
823 J., Lewis, S., Phillips, O. L. and Lloyd, J.: Structural, physiognomic and above-ground AGB variation in  
824 savanna-forest transition zones on three continents - How different are co-occurring savanna and forest  
825 formations?, *Biogeosciences*, 12(10), 2927–2951, doi:10.5194/bg-12-2927-2015, 2015.

826 Verberne, E. L. J., Hassink, J., De Willigen, P., Groot, J. J. R. and Van Veen, J. A.: Modelling  
827 organic matter dynamics in different soils, *Netherlands J. Agric. Sci.*, 38, 221–238, 1990.

828 Vourlitis, G. L., de Lobo, F. A., Lawrence, S., de Lucena, I. C., Pinto, O. B., Dalmagro, H. J.,  
829 Ortiz, C. E. and de Nogueira, J. S.: Variations in Stand Structure and Diversity along a Soil Fertility  
830 Gradient in a Brazilian Savanna (Cerrado) in Southern Mato Grosso, *Soil Sci. Soc. Am. J.*, 77(4), 1370–  
831 1379, doi:10.2136/sssaj2012.0336, 2013.

832 Wang, S., Huang, J., He, Y. and Guan, Y.: Combined effects of the Pacific Decadal Oscillation  
833 and El Niño-Southern Oscillation on Global Land Dry–Wet Changes, *Sci. Rep.*, 4, 6651,  
834 doi:10.1038/srep06651, 2014.

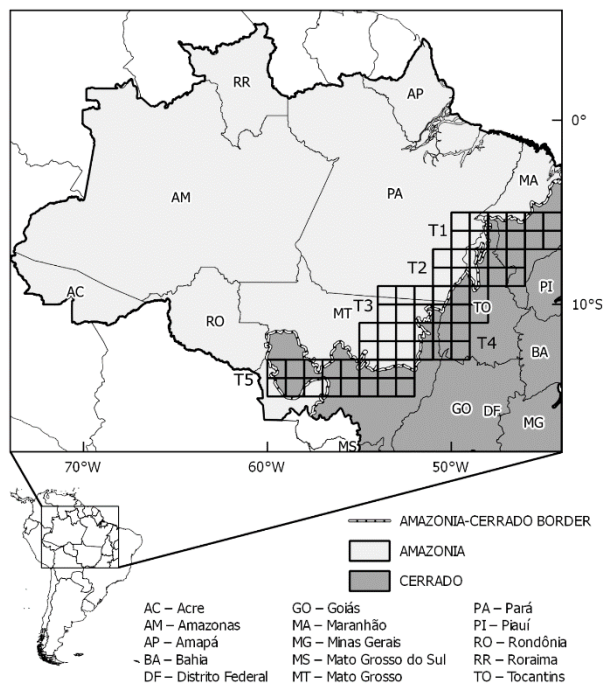
835 Yang, X. and Post, W. M.: Phosphorus transformations as a function of pedogenesis: A synthesis  
836 of soil phosphorus data using Hedley fractionation method, *Biogeosciences*, 8, 2907–2916,  
837 doi:10.5194/bg-8-2907-2011, 2011.

838 Yang, X., Post, W. M., Thornton, P. E. and Jain, A.: The distribution of soil phosphorus for global  
839 biogeochemical modeling, *Biogeosciences*, 10, 2525–2537, doi:10.5194/bg-10-2525-2013, 2013.

840            Yang, X., Thornton, P. E., Ricciuto, D. M. and Post, W. M.: The role of phosphorus dynamics in  
841 tropical forests - A modeling study using CLM-CNP, *Biogeosciences*, 11, 1667–1681, doi:10.5194/bg-  
842 11-1667-2014, 2014.

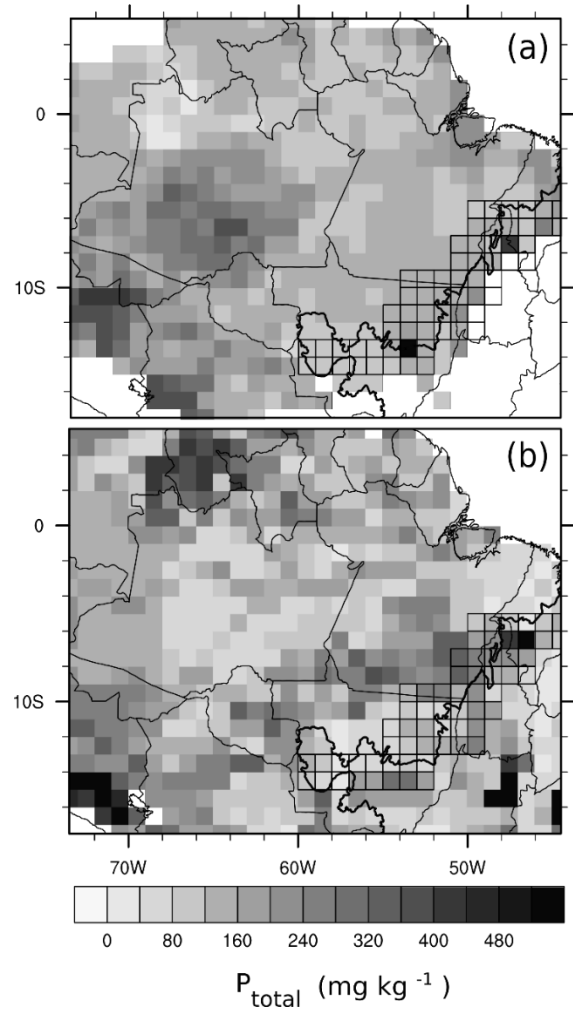
843

844



845

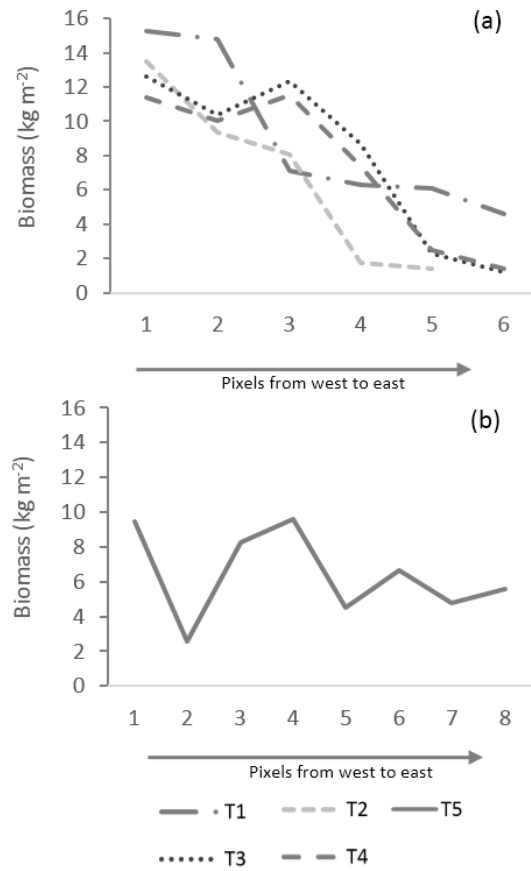
846 **Figure 1.** Delimitation of the study area Amazonia (in light gray) and Cerrado (in dark gray) (IBGE,  
 847 2004), and the location of five transects used in this work (from T1 to T5). The dashed line represents the  
 848 border between biomes.



849

850 **Figure 2.** (a) Map of regional total P in the soil (PR), (b) Map of global total P in the soil (Yang et al.,  
 851 2013) (PG).

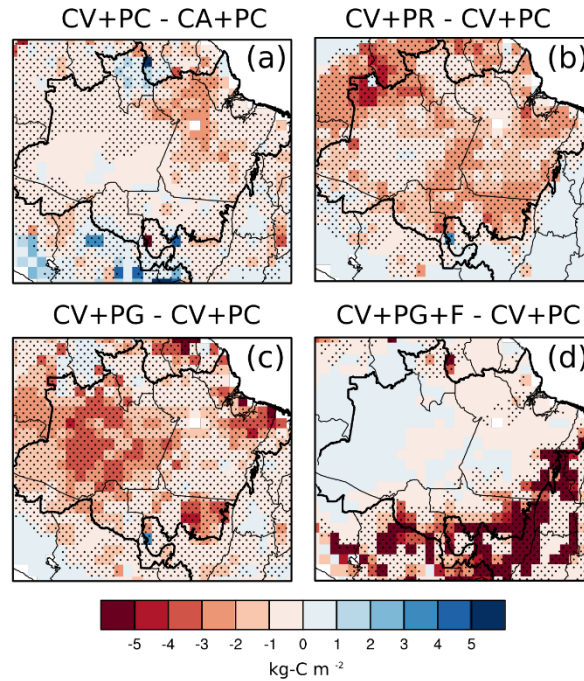
852



853

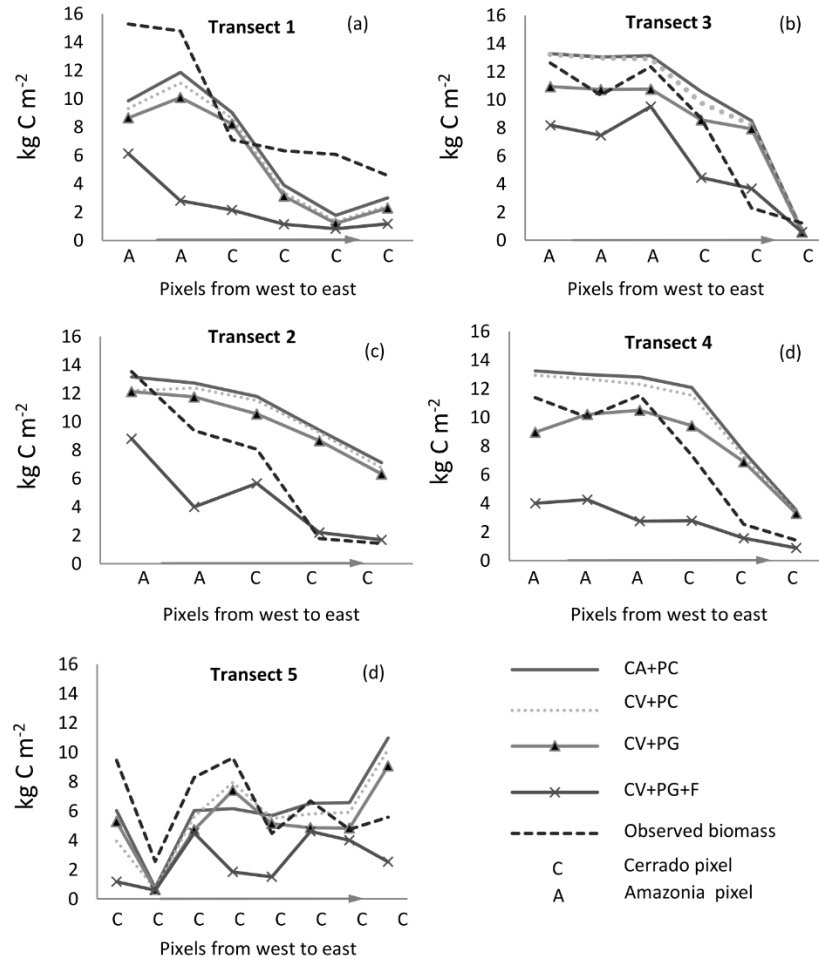
854 **Figure 3.** Average variations of AGB in pixels from West to East in the Amazonia-Cerrado transition

855 for transects T1, T2, T3 and T4 (a), and T5 (b).



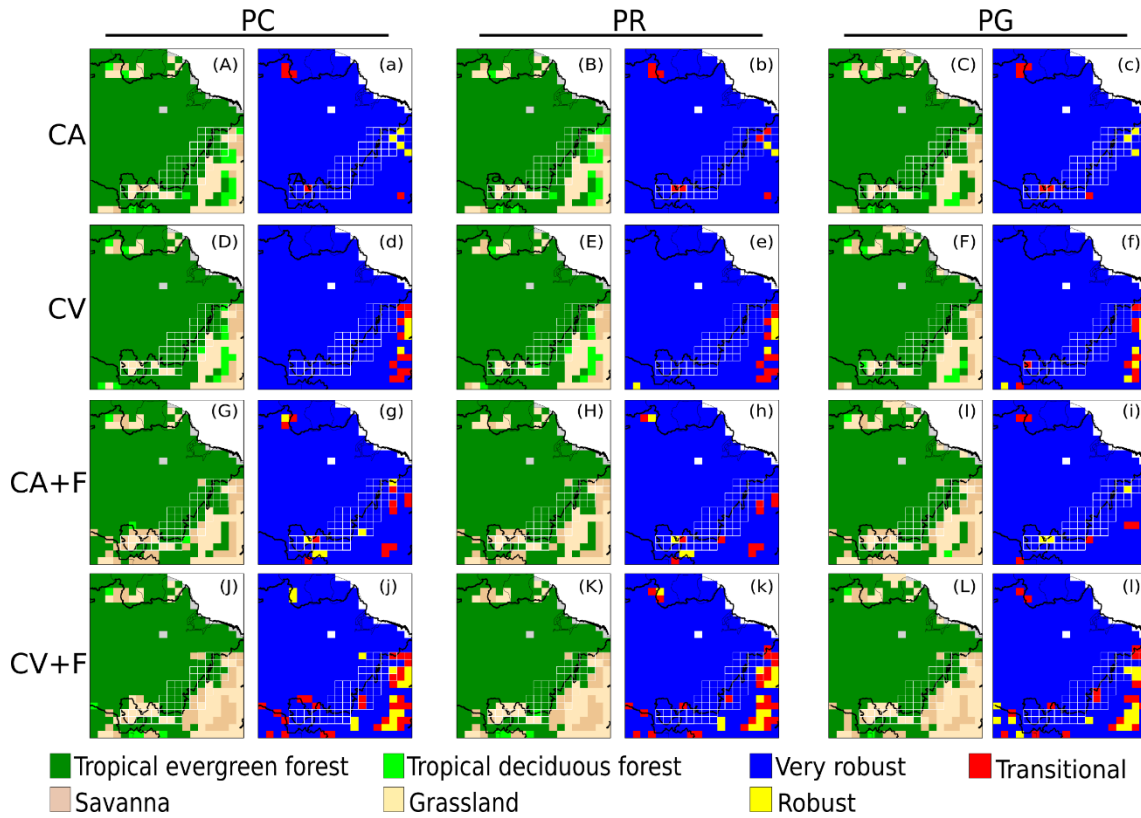
856

857 **Figure 4.** Effects of inter-annual climate variability (a), Regional P limitation (b), Global P limitation (c),  
 858 and fire (d) on AGB. The hatched areas indicate that the variables are significantly different compared to  
 859 the control simulation at the level of 95% according to the t-test. The thick black line is the geographical  
 860 limits of the biomes.



861

862 **Figure 5.** Average longitudinal AGB gradient in Amazonia-Cerrado transition simulated for T1 to T5  
 863 considering different combinations: observed data; seasonal climate control simulation (CA+PC); inter-  
 864 annual climate variability (CV+PC); inter-annual climate variability + global P limitation (CV+PG); and  
 865 inter-annual climate variability + P + fire occurrence (CV+PG+F).



867

868 **Figure 6.** Results for the dominant vegetation cover simulated by INLAND for the different treatments

869 (A-L) and a metric of variability of results (a-l). Simulations are considered very robust if the dominant

870 vegetation agrees on 9-10 of the last 10 years of simulation, robust if it agrees on 7-8 years, and

871 transitional if on 6 or fewer years.

872

873



874 **Table 1.** Simulations with different scenarios evaluated by INLAND model in Amazonia-Cerrado  
 875 transition. CA, climatological average, 1961-1990; CV, monthly climate data, 1948-2008; the nutrient  
 876 limitation on  $V_{\max}$  - PC, no P limitation ( $V_{\max} = 65 \mu\text{mol-CO}_2 \text{ m}^{-2} \text{ s}^{-1}$ ); PR, regional P limitation; PG,  
 877 global P limitation).

Climate	CO <sub>2</sub>	Fire (F)	$V_{\max}$		
			PC	PR	PG
CA	Variable	Off	CA+PC	CA+PR	CA+PG
CA	Variable	On	CA+PC+F	CA+PR+F	CA+PG+F
CV	Variable	Off	CV+PC	CV+PR	CV+PG
CV	Variable	On	CV+PC+F	CV+PR+F	CV+PG+F

878

879

880 **Table 2.** Individual and combined effects for each simulation in Amazonia-Cerrado transition. CA,  
 881 climatological seasonal average, 1961-1990; CV, monthly climate data, 1948-2008; the nutrient limitation  
 882 on  $V_{\max}$  - PC, no P limitation ( $V_{\max} = 65 \mu\text{molCO}_2 \text{ m}^{-2} \text{ s}^{-1}$ ); PR, regional P limitation; PG, global P  
 883 limitation)

Climate (C)	Phosphorus (P)	Fire (F)
(CV+PC)-(CA+PC)	(CA+PR)-(CA+PC)	(CA+PC+F)-(CA+PC)
(CV+PR)-(CA+PR)	(CV+PR)-(CV+PC)	(CV+PC+F)-(CV+PC)
(CV+PG)-(CA+PG)	(CA+PG)-(CA+PC)	(CA+PR+F)-(CA+PR)
	(CV+PG)-(CV+PC)	(CV+PR+F)-(CV+PR)
		(CA+PG+F)-(CA+PG)
		(CV+PG+F)-(CV+PG)

884

885

886 **Table 3.** Summary of average NPP, LAI and AGB for the Amazonia-Cerrado transition at the transects  
887 domains, considering all simulations with CA and CV regardless of fire presence or P limitation. The  
888 results of a one-way ANOVA are also shown, including the *F* statistic, and *p* value. Values within each  
889 column followed by a different letter are significantly different ( $p < 0.05$ ) according to the Tukey–Kramer  
890 test ( $n=1860$ : 31 pixels x 10 years x  $n_{\text{simulation}/2}$ ).

<b>Group 1</b>	<b>NPP</b>		<b>LAI<sub>total</sub></b>		<b>LAI<sub>lower</sub></b>		<b>LAI<sub>upper</sub></b>		<b>AGB</b>	
	kg-C m <sup>-2</sup> yr <sup>-1</sup>		m <sup>2</sup> m <sup>-2</sup>		m <sup>2</sup> m <sup>-2</sup>		m <sup>2</sup> m <sup>-2</sup>		kg-C m <sup>-2</sup>	
CA	0.68	a	7.47	a	1.98	a	5.49	a	6.68	a
CV	0.64	b	7.15	b	2.11	a	5.04	b	6.30	b
<i>F</i>	40.2		57.2		2.96		36.0		11.3	
<i>p</i>	<0.001		<0.001		<i>ns</i>		<0.01		<0.001	

891

892

893 **Table 4.** Summary of average NPP, LAI and AGB for the transition at the transects domains, considering  
894 different P limitation, regardless of climate and fire presence. The results of a one-way ANOVA are also  
895 shown, including the *F* statistic, and p value. Values within each column followed by a different letter are  
896 significantly different ( $p < 0.05$ ) according to the Tukey–Kramer test ( $n=1240$ : 31 pixels x 10 years x  
897  $n_{\text{simulation}/3}$ ).

<b>Group 2</b>	<b>NPP</b>		<b>LAI<sub>total</sub></b>		<b>LAI<sub>lower</sub></b>		<b>LAI<sub>upper</sub></b>		<b>AGB</b>	
	kg-C m <sup>-2</sup> yr <sup>-1</sup>		m <sup>2</sup> m <sup>-2</sup>		m <sup>2</sup> m <sup>-2</sup>		m <sup>2</sup> m <sup>-2</sup>		kg-C m <sup>-2</sup>	
PC	0.71	a	7.64	a	1.84	b	5.80	a	7.15	a
PR	0.64	b	7.15	b	2.19	a	4.95	b	6.20	b
PG	0.64	b	7.14	b	2.10	a	5.04	b	6.12	b
<i>F</i> <sub>2,99</sub>	62.8		61.0		8.75		53.5		33.6	
<i>p</i>	<0.001		<0.001		<0.01		<0.01		<0.001	

898

899

900 **Table 5.** Summary of average NPP, LAI and AGB for the transition at the transects domains, considering  
 901 presence or absence of fire. The results of a one-way ANOVA are also shown, including the *F* statistic,  
 902 and p value. Values within each column followed by a different letter are significantly different ( $p < 0.05$ )  
 903 according to the Tukey–Kramer test ( $n=1860$ : 31 pixels x 10 years x  $n_{\text{simulation}/2}$ ).

<b>Group 3</b>	<b>NPP</b>		<b>LAI<sub>total</sub></b>		<b>LAI<sub>lower</sub></b>		<b>LAI<sub>upper</sub></b>		<b>AGB</b>	
	kg-C m <sup>-2</sup> yr <sup>-1</sup>		m <sup>2</sup> m <sup>-2</sup>		m <sup>2</sup> m <sup>-2</sup>		m <sup>2</sup> m <sup>-2</sup>		kg-C m <sup>-2</sup>	
Fire OFF	0.66	a	6.72	b	0.88	b	5.84	a	8.47	b
Fire ON	0.67	b	7.90	a	3.21	a	4.69	b	4.51	a
<i>F</i> <sub>3,84</sub>	8.28		937		1459		249		1719	
<i>p</i>	<0.005		<0.001		<0.01		<0.01		<0.001	

904

905

906 **Table 6.** Summary of average NPP, LAI and AGB for the transition at the transects domains, considering  
 907 all factor combinations. The results of a one-way ANOVA are also shown, including the *F* statistic, and  
 908 *p* value. Values within each column followed by a different letter are significantly different ( $p < 0.05$ )  
 909 according to the Tukey–Kramer test (n=310: 31 pixels x 10 years).

	<b>NPP</b>		<b>LAI<sub>total</sub></b>		<b>LAI<sub>lower</sub></b>		<b>LAI<sub>upper</sub></b>		<b>AGB</b>	
	kg-C m <sup>-2</sup> yr <sup>-1</sup>		m <sup>2</sup> m <sup>-2</sup>		m <sup>2</sup> m <sup>-2</sup>		m <sup>2</sup> m <sup>-2</sup>		kg-C m <sup>-2</sup>	
CV+PC	0.69	bcd	6.96	d	0.84	e	6.48	a	9.01	ab
CV+PG	0.61	f	6.24	f	0.85	e	5.60	bc	7.91	c
CV+PR	0.62	f	6.33	f	0.85	e	5.74	bc	8.04	c
CV+PC+F	0.69	abc	7.92	b	2.91	cd	4.61	ef	4.89	de
CV+PG+F	0.63	ef	7.76	b	3.73	a	5.81	bc	3.91	f
CV+PR+F	0.63	ef	7.65	bc	3.47	ab	4.69	ef	4.02	f
CA+PC	0.72	ab	7.39	c	0.91	e	6.12	ab	9.31	a
CA+PG	0.64	def	6.64	e	0.91	e	5.40	cd	8.22	c
CA+PR	0.65	cdef	6.72	de	0.91	e	5.49	cd	8.31	bc
CA+PC+F	0.74	a	8.29	a	2.69	d	5.02	de	5.40	d
CA+PG+F	0.67	cde	7.90	b	3.29	abc	4.04	g	4.45	ef
CA+PR+F	0.67	cde	7.88	b	3.19	bc	4.18	fg	4.42	ef
<i>F</i>	16.2		115		140		38.1		172	
<i>p</i>	<0.001		<0.001		<0.01		<0.01		<0.001	

910

911 **Table 7.** Correlation coefficients of AGB simulated by INLAND and field estimates (n= 310: 31 pixels  
 912 x 10 years).

	<b>T1</b>	<b>T2</b>	<b>T3</b>	<b>T4</b>	<b>T5</b>	<b>All transects</b>
CA+PC	0.843	0.928	0.886	0.937	0.337	0.786
CV+PC	0.838	0.884	0.890	0.939	0.355	0.781
CA+PR	0.793	0.848	0.830	0.911	0.399	0.756
CV+PR	0.795	0.793	0.832	0.907	0.527	0.771
CA+PG	0.814	0.951	0.838	0.889	0.388	0.776
CV+PG	0.825	0.922	0.840	0.879	0.496	0.792
CA+PC+F	0.988	0.987	0.977	0.892	0.133	0.795
CV+PC+F	0.976	0.947	0.933	0.908	0.187	0.790
CA+PR+F	0.842	0.805	0.981	0.808	0.561	0.799
CV+PR+F	0.925	0.804	0.927	0.808	0.319	0.757
CA+PG+F	0.844	0.961	0.980	0.830	0.430	0.809
CV+PG+F	0.845	0.932	0.931	0.881	0.177	0.753
CA avg	0.854	0.913	0.915	0.878	0.375	0.787
CV avg	0.867	0.880	0.892	0.887	0.344	0.774

913